THE ASTROPHYSICAL JOURNAL, 559:791–811, 2001 October 1

GALAXY POPULATIONS AND EVOLUTION IN CLUSTERS. I. DYNAMICS AND THE ORIGIN OF LOW-MASS GALAXIES IN THE VIRGO CLUSTER

CHRISTOPHER J. CONSELICE,[1,2] AND JOHN S. GALLAGHER III[1]
Department of Astronomy, University of Wisconsin, Madison

AND

ROSEMARY F. G. WYSE
Department of Physics and Astronomy, The Johns Hopkins University
Received 2000 November 20; accepted 2001 June 1

ABSTRACT

Early-type dwarfs are the most common galaxy in the local universe, yet their origin and evolution remain a mystery. Various cosmological scenarios predict that dwarf-like galaxies in dense areas are the first to form and hence should be the oldest stellar systems in clusters. By using radial velocities of early-type dwarfs in the Virgo cluster we demonstrate that these galaxies are not an old cluster population but have signatures of production from the infall of field galaxies. Evidence of this includes the combined large dispersions and substructure in spatial and kinematic distributions for Virgo early-type dwarfs and a velocity dispersion ratio with giant ellipticals expected for virialized and accreted populations. We also argue that these galaxies cannot originate from accreted field dwarfs, but must have physically evolved from a precursor population, of different morphology, that fell into Virgo some time in the past.

Subject headings: galaxies: dwarf — galaxies: elliptical and lenticular, cD — galaxies: evolution — galaxies: formation — galaxies: star clusters

1. INTRODUCTION

Early-type dwarfs are the most common galaxies in the local universe, yet we know very little about them (see Gallagher & Wyse 1994; Ferguson & Binggeli 1994). This is due to their very low luminosities and surface brightnesses hindering any detailed studies. Luminosity functions of nearby clusters show that faint galaxies[3] are by far more common than brighter galaxies (e.g., de Propris et al. 1995; Secker, Harris, & Plummer 1997; Trentham 1997; Phillipps et al. 1998). Additionally, in comparison to the field, galaxy clusters have steeper luminosity functions dominated by dE-like galaxies (e.g., Ferguson & Sandage 1989; de Propris et al. 1995; Secker et al. 1997; Marzke & da Costa 1997; Phillipps et al. 1998; Mobasher & Trentham 1998). How these objects originated and continue to exist in large numbers in clusters is presently a mystery.

A very basic question to ask is: where did these cluster dwarf galaxies come from? Do they have an origin similar to the dwarf elliptical and spheroidal galaxies seen in groups such as the Local Group (see Mateo 1998; van den Bergh 2000)? One basic difference between group and cluster dwarfs is the way they are distributed. In groups of galaxies, dwarf spheroidals are for the most part clustered around giants (Mateo 1998; Grebel 2000). However, in clusters dwarfs are in general *not* distributed around the giants, but follow the general potential (e.g., Binggeli, Tarenghi, & Sandage 1990; Ferguson 1992; Secker et al. 1997). In other respects, such as surface brightness, magnitude, and color, bright dEs in clusters have properties similar to bright Local Group dEs (Bothun et al. 1985; James 1991; Held & Mould 1994; Phillipps et al. 1998).

Dwarfs in rich clusters are faint and hard to identify, and as a result they were not discovered until Reeves (1956, 1977) and Hodge (1959, 1960, 1965) studied them in the Virgo and Fornax clusters. Since then many observations, conducted at various wavelengths and employing various techniques, have been applied to cluster dwarfs, with particular activity in the 1980s. Many of these studies were mainly interested in determining the galaxy luminosity functions in clusters (Ferguson & Sandage 1988; Phillipps et al. 1998; Mobasher & Trentham 1998; Trentham 1998) and not necessarily in the properties of the dwarf galaxies themselves. Luminosity functions are important for cosmology and galaxy formation theories, but they also reveal what the relative number densities of cluster dwarfs are in comparison with the field.

There are at least four different ideas for explaining where dEs seen in Virgo and other galaxy clusters originate. These are the following: (1) dEs are old primordial galaxies that formed early in the Virgo protocluster (e.g., White & Frenk 1991; Ostriker 1993; Farooqui 1994) and have survived in the cluster environment for several Gyr. (2) dEs are the passively evolved compact blue and emission-line galaxies seen at redshifts $z \sim 1$ (e.g., Babul & Rees 1992; Koo et al. 1995, 1997). (3) dEs are stripped and "harassed" spirals accreted into clusters, creating a morphological transformation: spiral → dE (Mao & Mo 1998; Moore, Lake, & Katz 1998; Moore et al. 1999). (4) dEs evolved from dwarf irregulars (Lin & Faber 1983). Alternatively dwarf ellipticals may form though a combination of these scenarios.

Solution (4) was considered quite seriously and given much attention in the 1980s but has since been largely discarded (e.g., Bothun et al. 1986; Gallagher & Hunter 1989) because of the problem of explaining large populations of

[1] Visiting Astronomer, Kitt Peak National Observatory, National Optical Astronomy Observatories, which is operated by the Association of Universities for Research in Astronomy, Inc. (AURA) under cooperative agreement with the National Science Foundation.

[2] Also: Space Telescope Science Institute, 3700 San Martin Drive, Baltimore, MD 21218.

[3] For the purposes of this paper, we refer to these objects as dwarfs. We further subdivide dwarfs into dwarf ellipticals (dE) and irregulars (dIrr). Dwarf spheroidals are not used as a separate term in this paper but are included in the dwarf elliptical class. The differences between dEs and dIrr will be discussed in § 2.1.

dEs that are more massive, brighter, and more compact than typical dwarf irregulars. Since any evolution from dIrr to dE requires fading, bright dEs cannot be accounted for by this evolution.

Possibility (2) was inspired by the large numbers of faint blue galaxies seen in redshift surveys (Babul & Rees 1992). These blue galaxies have low masses, similar to the masses of dwarfs (Koo et al. 1995). If no further star formation occurs then the magnitudes and surface brightnesses of these objects would be similar to those of dwarf ellipticals (Koo et al. 1995), thus allowing for the possibility of an evolutionary connection. However, there are several potential problems with this idea, the most important being the fact that many Local Group dwarf ellipticals contain several episodes of star formation (Mateo 1998) and hence have not evolved passively. A second problem is that the faint blue galaxies are a field population, yet in the nearby universe most dEs are in clusters. Third, some Virgo dEs are brighter than the luminosity to which these high-redshift, star-forming galaxies would evolve with no further star formation. Thus, a strictly passive evolution from a burst of star formation at $z \sim 1$ to the present cannot account for cluster dEs.

In this paper, we mainly address, and try to distinguish between, possibilities (1) and (3). The hypothesis we test is that cluster dEs either form by the galaxy harassment scenario (e.g., Moore et al. 1998) or are an old cluster population. These models depend upon a very active source of accreted galaxies to account for the large population of dEs in clusters. For the harassment idea to be correct, there must be signatures that dEs were accreted and underwent mass stripping, or that a large population of spirals existed in the protocluster. Modern Virgo spirals have properties that suggest they have recently been accreted (Huchra 1985), and this process likely occurred in the past as well. Harassment has also been used to explain the morphological transformation of Butcher-Oemler galaxies seen at moderate cluster redshifts ($z \approx 0.8$) into modern dwarf galaxies (Moore et al. 1996). A galaxy in a cluster, such as Virgo, interacts weakly with the other cluster members because of the high relative velocities between systems. Stars in the outer parts of accreted galaxies are stripped away as a result ot the increase of internal energy from impulsive interactions, and at the same time gas is stripped by ram pressure (Lee, Richer, & McCall 2000; Mori & Burkert 2000). Over the 1 Gyr orbital time the galaxy begins to lose its stars and gas, and over a longer time it can become a spheroidal system (Moore et al. 1998). Before a galaxy is stripped any gas it contains can become compressed by cluster tides, producing a starburst. Harassment does not differentiate between accreted galaxies and cluster members or galaxies on isotropic or anisotropic orbits. This theory predicts that the larger spiral galaxies become S0s (Moore et al. 1999) while the smaller ones will eventually resemble dwarf ellipticals. It remains to be determined, but seems unlikely, whether it is possible that each dE originated from a spiral. The increase in number of star-forming galaxies in $z \sim 1$ clusters may not need an explanation from an increase in the infall rate, since the field is rich in starbursts at this same redshift (e.g., Sullivan et al. 2000).

One way to test if cluster dEs originated from a relatively recently accreted population is to determine how their velocity and spatial distributions compare to those of giant ellipticals and spirals. The one-dimensional velocity dispersions of clusters are typically less than 1000 km s^{-1} (for Virgo the value is about 700 km s^{-1}). From radial velocity studies of Virgo galaxies it is known that the dispersion of the spiral population is higher and has a flatter distribution (less relaxed) than that of the ellipticals, which is Gaussian, an expected form for a relaxed population (e.g., Huchra 1985; Schindler, Binggeli, & Böhringer 1999, hereafter SBB99). This velocity distribution difference is usually interpreted as a consequence of the infall of spiral galaxies. As a very basic test we can measure the velocity and spatial distributions of Virgo dwarf galaxies to determine whether they have such accretion signatures, or instead signatures of an older relaxed cluster population. Furthermore, we can compare these distributions to various predictions, including the effects of relaxation, virialization, equipartition and dynamical friction.

We show that the early type dwarfs in Virgo, as well as all Virgo galaxies except ellipticals, have no strong signs of relaxation. Based on both their velocity and spatial distributions, we demonstrate that most Virgo dEs cannot have existed in Virgo for as long as the giant ellipticals have. The kinematic properties of Virgo dwarf ellipticals also suggest that these galaxies originate from an accreted component, whose infall rate peaked some time in the past. This paper is organized as follows: § 2 describes the observations and data, § 3 gives our results, § 4 describes various dynamical models, § 5 is a discussion of our results, and finally § 6 gives a summary. A Virgo cluster distance of 18 Mpc is used throughout, where $6^\circ = 1.9$ Mpc.

2. DATA AND OBSERVATIONS

The Virgo Cluster of galaxies is the nearest rich cluster, presenting both advantages and problems for studying its galaxies and structure. It is close enough so that its galaxies can be studied in detail, but because it is so close, it is spread out over 10° in the sky, making multiplexed observations of its galaxies time consuming.

Measuring radial velocities of faint, low surface brightness dwarf galaxies is also technically very challenging. The brightest dwarfs can be studied with little difficulty, but the fainter ones, with surface brightnesses significantly fainter than the night sky, though very numerous in Virgo, are difficult to observe spectroscopically. As such we can only determine radial velocities of relatively bright dEs. Previous to this work, the last published radial velocity catalog of Virgo contained 91 dE + dS0 galaxies (Binggeli, Popescu, & Tammann 1993). We increase the total number to 142 by measuring new velocities and combining these with previously published values.

We undertook radial velocity observations of selected Virgo galaxies with the Hydra multiobject spectrograph on the WIYN 3.5 m telescope and with the RC long-slit spectrograph on the Kitt Peak National Observatory 4 m telescope.

Hydra contained 95 fibers at the time these observations were made in 1999 April and 2000 March. For these observations Hydra's fibers fed the bench spectrograph with a 400 lines mm^{-1} grating during 1999 April and the 600 lines mm^{-1} grating in 2000 March. Total dispersions of 2.1 Å $pixel^{-1}$ and 1.4 Å $pixel^{-1}$ and equivalent resolutions of 6.9 and 4.6 Å were obtained for the two gratings respectively, giving a typical error of 35–50 km s^{-1} in radial velocity. The wavelength ranges for the 1999 April and 2000 March runs were $\lambda\lambda$3400–7600 and $\lambda\lambda$3900–6700. In both runs we used the 3″ diameter Hydra blue fibers. The field of view of Hydra is approximately 1°.

We observed a total of three fields over the course of three nights in 1999 and the same number of fields in 2000. Radial velocities were obtained in three different areas of the cluster; roughly the central part (near M87) as well as the northern ($\delta = 13°$: near M86) and southern clumps ($\delta = 7°$: near M49). Sample selection was done using digitized Palomar sky survey plates, in conjunction with morphological classifications from the Binggeli, Sandage, & Tammann (1985) Virgo Cluster Catalog (hereafter VCC). Each fiber setup contained between 15 and 25 galaxies, with most of the remaining fibers positioned on the sky across each field. Some Hydra fibers that could not be assigned to dEs were placed on nondwarf Virgo galaxies whose redshifts were unknown. Total exposure time for each field was typically about 11,000 s. We bias subtracted, flat-fielded and then wavelength-calibrated the spectra with a Helium-Neon-Argon lamp. All reduction procedures, except the basic CCD processing, occurred using the IRAF task *dohydra*. We then combined each of the individual frames and later sky-subtracted galaxy fibers using the closest sky fibers to each object. Sky subtraction was typically successful with an effective removal of the sky continuum and telluric emission features, with occasional residual sky lines in the red part of the spectrum. These remaining faint sky lines, typically in the region near 7000 Å, were removed by hand.

Long-slit data from the KPNO 4 m telescope were used to determine the radial velocities of two dwarf ellipticals in 1999 June. The RC spectrograph with the KP-007 grating was used, giving a dispersion of 1.4 Å pixel^{-1} and a wavelength coverage $\lambda\lambda$4400–7350. These spectra were reduced and extracted using the APALL program in the IRAF long-slit package.

During these observations we obtained spectroscopy of velocity standards to calibrate the velocity zero point. The stars observed are listed in Table 1; most are G–K spectral types. Each stellar spectrum was reduced and calibrated the same way as were the galaxy spectra. For each night we create a single velocity template by combining the spectrum of each star observed, using the task *sumspec* in the RVSAO (Radial Velocity Smithsonian Astrophysical Observatory) package.

Using these standards, we then computed the radial velocities for our complete sample of observed objects. Only a fraction, ~25%, of the observed galaxies had high enough signal-to-noise (S/N) ratios for a reliable radial velocity measurement. Figure 1 shows a typical Hydra dE spectrum. We determine velocities by cross-correlating absorption

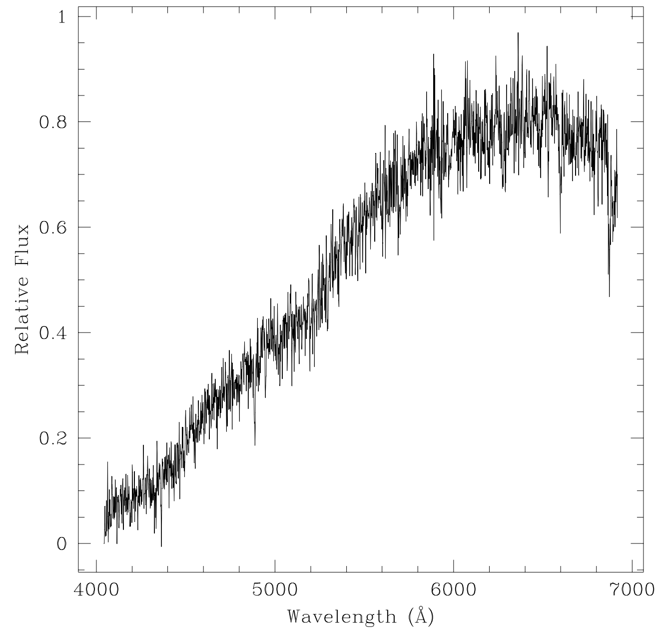

FIG. 1.—Typical WIYN Hydra Multi-Object Spectrograph spectrum of a dwarf elliptical.

features with the velocity template using the *xcsao* task in the RVSAO 2.0 package within the IRAF environment (Kurtz & Douglas 1998). *Xcsao* outputs a radial velocity for each object computed from cross-correlation fits, including a quality R-value (Tonry & Davis 1979), where a higher value of R indicates a better fit, and we adopt $R \geq 3$ as the limit of reliability (Kurtz & Douglass 1998). Of those observed, 43 have high enough S/N and R values greater than 3 for a reliable radial velocity measurement, and 37 of these are dwarf ellipticals or dwarf lenticulars. In Figure 2 we plot the difference between our computed velocities with published radial velocities for those few galaxies with previously measured values. The average absolute difference between our measured velocities and those previously published is 128 ± 71 km s^{-1}. All new velocities are shown in Table 2, while Table 3 lists all Virgo dEs with known radial velocities.

We combine our new velocity measurements with previously published ones. The most recent previous studies on the dynamical properties of the Virgo cluster, Binggeli et al. (1993) and SBB99 contained 385 and 403 velocities respectively. The present study uses 497 velocities, with new velocities mainly of faint galaxies, taken from a variety of sources including Drinkwater et al. (1996) and Grogin,

TABLE 1

VELOCITY STANDARDS

Name	R.A. (J2000)	Decl. (J2000)	Spectral Type	Velocity (km s^{-1})
HD 29139	04 35 55.2	+16 30 33.5	K5III	54.1
HD 62509	07 45 19.0	+28 01 34.3	K0IIIb	3.3
HD 84441	09 45 51.1	+23 46 27.3	G1II	4.8
HD 135722......	15 15 30.2	+33 18 53.4	G8III	−12.3
HD 136512......	15 20 08.6	+29 36 58.4	K0III	−53.1
HD 137422......	15 20 43.7	+71 50 02.5	A3III	−3.9

NOTE.—Units of right ascension are hours, minutes, and seconds, and units of declination are degrees, arcminutes, and arcseconds.

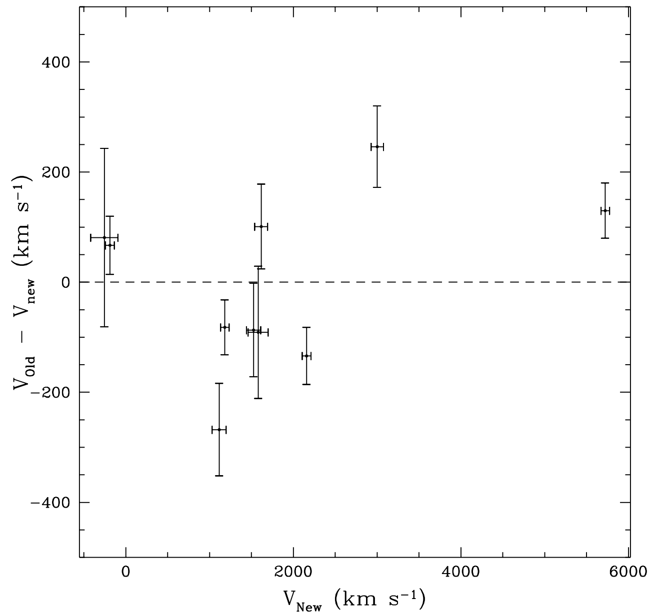

FIG. 2.—Difference between previously derived radial velocities and values measured in this study.

Geller, & Huchra (1998). The distribution across Virgo of all the galaxies used in our analysis is shown in Figure 3.

2.1. *Galaxy Morphology and Populations*

Identifying a morphological type for a galaxy, or for our purposes, identifying members of distinct populations, is never a simple or straightforward procedure. In Virgo the problem is even greater owing to the poor correlation of Hubble types with global properties such as star formation rates (Koopmann & Kenney 1998). A morphological classification therefore has its limitations. Nonetheless, we characterize seven distinct galaxy populations for this study based on morphology alone. These are classical ellipticals (E), lenticulars (S0), spirals (Sa–Sd), irregulars (Irr, I, dIrr, Sm, blue compact dwarfs), dwarf ellipticals (dE, dSph), nucleated dwarf ellipticals (dE, N), and dwarf lenticulars (dS0). We often combine dwarf ellipticals and dwarf nucleated ellipticals into one class, which we denote as the total dwarf ellipticals (dET).

Almost all of the morphological types are taken from the Virgo Cluster Catalog (VCC). Some galaxies in this paper are unclassified in the VCC catalog, particularly in the region $12^h50^m00^s$–$13^h15^m00^s$. We either classified these galaxies ourselves, using second generation Palomar Sky Survey images, or adopted classifications from other published studies. If there was a significant uncertainty in a galaxy's morphological type, we assigned no classification and the galaxy was left out of the analysis involving galaxy populations. The morphological identifications of Virgo core galaxies (defined in the next section) with radial velocities breaks down as follows: 40 ellipticals, 56 S0s, 18 dEs, 79 nucleated dEs, 28 dS0s, 81 irregulars, and 119 spirals.

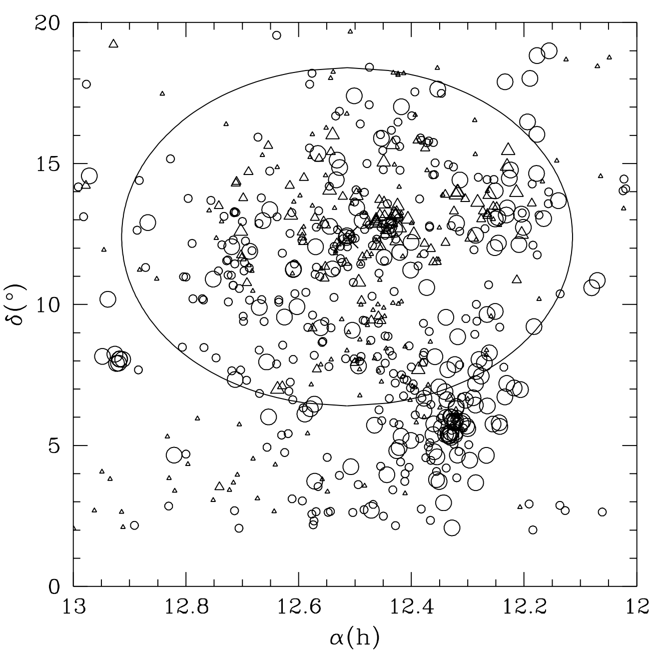

FIG. 3.—Projected distribution (J2000) of Virgo galaxies with known radial velocities. The large cross represents the location of the large elliptical M87. The 6° circle represents the spatial area used to define the Virgo core sample. The different points for galaxies represent different velocities. The larger the symbol, the larger the difference from 1000 km s^{-1}, with triangles for $V < 1000$ km s^{-1}, and circles for $V > 1000$ km s^{-1}.

3. RESULTS

3.1. *Virgo Cluster: Structure*

Smith (1936) was the first to study the dynamical structure of the Virgo cluster based on 32 radial velocities obtained by himself, V. M. Slipher, and M. L. Humason (unpublished). Using this data, Smith (1936) concluded that the Virgo cluster is a bound system and derived a mass for it using the kinematics of these galaxies. This provided some of the first evidence for extensive dark matter in clusters, similar to the pioneering study of Coma done by Zwicky (1933). This derived mass assumed that the cluster components are virialized; however, the Virgo cluster is not as indicated by the presence of subclusters, which have been known since the study of de Vaucouleurs (1961). More detailed observations revealed Virgo to be a complex system of different aggregate clouds of galaxies that are part of the Local Supercluster (e.g., de Vaucouleurs 1961; Holmberg 1961; de Vaucouleurs & de Vaucouleurs 1973; Huchra 1985; Binggeli et al. 1987, 1993; SBB99). De Vaucouleurs & de Vaucouleurs (1973) identified and named several of these clouds, in the area of the Virgo cluster studied here (α (J2000): 12^h–13^h, δ (J2000): 0°– 20°; $v < 3000$ km s^{-1}). These are, using the de Vaucouleurs & de Vaucouleurs (1973) notation, the M cloud, the Wa and Wb clouds, and the Virgo I and II clusters. The W cloud (combined Wa and Wb) is the most distinct, with a well-defined locus at $\delta \sim 5°$ and velocities near 2600 km s^{-1}. The Virgo II cluster (the B cluster in Binggeli et al. 1987) is south of the area used in this study, but it and the other galaxy clouds near Virgo are probably merging with each other based on their relative positions and velocities.

These various clouds can bias results; thus to study the Virgo core cloud we define two separate regions. We define the "Virgo region" as those galaxies with α (J2000): 12^h–13^h, δ (J2000), 0°–20°, and with velocities $v < 3000$ km s^{-1}. The distribution of velocities for each of our defined galaxy populations is plotted in Figure 4. This is still a rather generous spatial and velocity coverage that is certainly unsatisfactory for studying only galaxies associated with the primary Virgo core region. To study only galaxies in the cluster proper we identify a separate Virgo "core" contain-

TABLE 2

NEW VIRGO CLUSTER RADIAL VELOCITIES

Name	R.A. (J2000.0)	Decl. (J2000.0)	Type[a]	Magnitude	v (km s^{-1})	R-value[b]
VCC 292	12 18 31.4	+05 51 09	dE1,N	17.0	2232 ± 66	3.2
VCC 300	12 18 42.2	+05 40 03	dE5	18.1	98541 ± 61	3.0
VCC 303	12 18 42.8	+05 47 27	dE2?,N	15.8	2846 ± 43	5.6
VCC 314	12 18 57.3	+06 11 05	SBc?	14.9	5724 ± 40	3.9
VCC 315	12 19 00.5	+06 05 40	SBa(s)	15.0	1525 ± 31	7.9
VCC 321	12 19 05.6	+05 44 27	dE6	18.0	1227 ± 73	3.3
VCC 323	12 19 06.4	+05 43 33	Sab	14.9	3002 ± 39	5.2
VCC 336	12 19 17.6	+05 52 39	dE,N	16.2	2990 ± 42	4.7
VCC 338	12 19 20.2	+05 28 00	dE3,N	16.5	2802 ± 53	4.3
VCC 362	12 19 42.2	+05 32 17	SB(s)a	14.6	1617 ± 40	5.6
VCC 366	12 19 45.3	+06 00 21	S0	15.0	2158 ± 41	7.3
VCC 390	12 20 04.4	+05 24 57	dE3	16.9	2479 ± 38	5.4
VCC 684	12 23 57.7	+12 53 13	dE,N	16.2	537 ± 58	4.7
VCC 719	12 24 19.0	+12 54 47	dE2	18.5	32738 ± 59	3.1
VCC 723	12 24 22.1	+13 01 37	dS0?	15.0	−111 ± 25	9.6
VCC 753	12 24 51.6	+13 06 40	dE,N	16.3	31166 ± 57	3.8
VCC 762	12 25 02.8	+07 30 23	dE3,N	15.3	1200 ± 25	6.7
VCC 765	12 25 03.5	+13 14 40	dE1,N	16.0	854 ± 36	6.8
VCC 781	12 25 15.0	+12 42 52	dS0,N	14.8	−188 ± 23	13.2
VCC 817	12 25 37.7	+15 50 06	dE1	15.0	1086 ± 57	3.4
VCC 838	12 25 46.9	+12 45 37	dE2	17.5	88564 ± 72	3.8
VCC 854	12 25 55.6	+12 46 11	dE8,N	17.3	684 ± 75	3.8
VCC 871	12 26 05.6	+12 33 34	dE,N	15.4	1636 ± 76	3.1
VCC 872	12 26 00.7	+12 51 40	dE0.N	17.0	1183 ± 50	3.7
VCC 896	12 26 22.5	+12 47 00	dE3,N	17.8	2114 ± 63	2.7
VCC 916	12 26 33.3	+12 44 24	dE,N	16.2	1115 ± 32	6.9
VCC 928	12 26 39.6	+12 30 48	dE?	16.2	−254 ± 54	4.9
VCC 967	12 27 04.0	+12 51 54	dE4	18.7	1135 ± 51	3.1
VCC 977	12 27 11.1	+12 02 18	dE4,N	17.9	102 ± 45	4.2
VCC 996	12 27 21.2	+13 06 36	dE5	18.4	−28 ± 32	7.7
VCC 1027......	12 27 38.0	+12 52 48	dE0,N	18.1	77 ± 46	5.2
VCC 1040......	12 27 44.5	+12 58 55	dE3,N	17.5	−143 ± 63	5.2
VCC 1042......	12 27 45.8	+12 52 19	dE4	18.6	−62 ± 13	19.4
VCC 1237......	12 29 51.2	+13 52 03		15.5	−255 ± 72	2.9
VCC 1351......	12 31 17.5	+13 49 42	dE4	16.0	187 ± 48	6.2
VCC 1870......	12 41 15.3	+11 17 55	dE6	15.8	1617 ± 27	8.7
VCC 1881......	12 41 29.5	+10 45 46	dE3,N	16.2	138 ± 56	3.9
VCC 1891......	12 41 48.9	+11 11 29	dE4,N	16.7	1016 ± 43	4.6
VCC 1919......	12 42 19.0	+10 34 04	dE0,N	17.0	1869 ± 54	3.2
VCC 1927......	12 42 35.9	+10 33 55	Sc	15.0	20199 ± 14	9.6
VCC 1948......	12 42 58.0	+10 40 55	dE3	15.1	1581 ± 22	9.8
VCC 1958......	12 43 10.0	+11 02 12	dE2,N	17.0	1049 ± 30	3.5
VCC 1971......	12 43 31.0	+11 02 50	dE3	16.6	1376 ± 34	6.1

NOTE.—Units of right ascension are hours, minutes, and seconds, and units of declination are degrees, arcminutes, and arcseconds.

[a] Morphological types are from the estimates given by Binggeli et al. 1985.

[b] See § 2 for explanation.

ing only galaxies within 6° of the center of the luminosity density of the Virgo I or A main cluster [defined by Binggeli et al. (1987) as (B1950) $12^{h}27^{m}50^{s}$, $+13°01'24''$] and with radial velocities $v < 2400$ km s^{-1}. Spatially these galaxies are found within the circle shown in Figure 3. Isolation of this sample allows us to perform statistical tests without a large bias or contamination from Local Supercluster clouds seen in projection toward the cluster, although some contamination is inevitable. The Virgo "core" velocity histograms are plotted in Figure 5; while the distribution of spatial positions of all likely members of Virgo, based on VCC estimates, are shown for each galaxy population in Figure 6. Figure 6 contains an essentially complete listing of all Virgo galaxies down to magnitude $B = 18$.

The analysis presented here is concerned only with these two areas in Virgo, but mostly with the Virgo core region. While our large sample of 497 radial velocities, 429 of which are in the Virgo core, permits a detailed dynamical study of the cluster and its neighboring clouds, we postpone an analysis of these clouds for another paper. It is sufficient for comparison purposes to state a few basic parameters (Table 4). The mean Virgo core heliocentric velocity is found to be 1064 ± 34 km s^{-1}, less than 0.5 σ from the value of 1050 ± 35 km s^{-1} found by Binggeli et al. (1993), and has a total velocity dispersion of 705 km s^{-1}, close to the 699 km s^{-1} dispersion found by Binggeli et al. (1993).

The usefulness of these mean and dispersion quantities is limited since as discussed above, the Virgo cluster is not a

TABLE 3

VIRGO DWARF ELLIPTICAL GALAXIES WITH RADIAL VELOCITIES

Name	Identification	R.A. (J2000.0)	Decl. (J2000.0)	Type[a]	Magnitude	v (km s^{-1})	Reference
VCC 9..........	IC 3019	12 09 22.3	+13 59 33	dE1,N	13.93	1804 ± 49	1
VCC 31		12 10 56.7	+09 13 07	dE	14.87	2215 ± 40	2
VCC 168		12 15 54.3	+14 01 26	dE2	17.0	682 ± 10	1
VCC 178	IC 3081	12 16 09.4	+12 41 26	dE5,N	15.10	1168 ± 53	1
VCC 200		12 16 33.9	+13 01 56	dE2,N	14.69	65 ± 43	2
VCC 216	IC 3097	12 17 01.2	+09 24 32	dE5,p,N	14.9	1325 ± 79	2
VCC 227	UGC 7314	12 17 14.4	+08 56 32	dE5,N.	14.90	1290 ± 91	2
VCC 230	IC 3101	12 17 19.5	+11 56 32	dE4,N	15.2	1398 ± 73	2
VCC 292		12 18 31.4	+05 51 09	dE1,N	17.0	2232 ± 66	3
VCC 303		12 18 42.8	+05 47 27	dE2?,N	15.8	2846 ± 43	3
VCC 319	IC 3142	12 19 01.7	+13 58 56	dE0,N	16.2	−206	4
VCC 321		12 19 05.6	+05 44 27	dE6	18.0	1227 ± 73	3
VCC 336		12 19 17.6	+05 52 39	dE4,N	16.2	2990 ± 42	3
VCC 338		12 19 20.2	+05 28 00	dE3,N	16.5	2802 ± 53	3
VCC 390		12 20 04.4	+05 24 57	dE3	16.9	2479 ± 38	3
VCC 397		12 20 12.2	+06 37 23	dE5,N	15.0	2495 ± 60	5
VCC 405		12 20 18.1	+05 59 57	dE0	20.0	2097	6
VCC 437	UGC 7399A	12 20 48.1	+17 29 16	dE5,N	14.54	1474 ± 46	2
VCC 542	IC 3218	12 22 19.6	+06 55 39	dE0,N	15.00	1057 ± 39	5
VCC 543	UGC 7436	12 22 19.5	+14 45 39	dE5	14.77	861 ± 58	2
VCC 545	IC 783A	12 22 19.6	+15 44 02	dE2,N	15.17	1159 ± 49	2
VCC 546		12 22 21.6	+10 36 07	dE6	15.7	2067 ± 104	7
VCC 608	NGC 4322	12 23 01.7	+15 54 21	dE4,N	14.70	1803 ± 100	2
VCC 634	NGC 4328	12 23 19.9	+15 49 13	dE1,N	14.24	499 ± 24	2
VCC 684		12 23 57.7	+12 53 13	dE0,N	16.2	537 ± 58	3
VCC 745	NGC 4366	12 24 47.0	+07 21 10	dE6,N	14.67	1286 ± 39	5
VCC 750		12 24 49.6	+06 45 33	dE5,N	15.0	1083 ± 38	5
VCC 762		12 25 02.8	+07 30 23	dE3,N	15.3	1200 ± 25	3
VCC 765		12 25 03.5	+13 14 40	dE1,N	16.0	854 ± 36	3
VCC 786	IC 3305	12 25 14.5	+11 50 57	dE7,N	15.11	2388 ± 30	2
VCC 790		12 25 17.5	+14 10 21	dE1,N	16.4	573 ± 54	8
VCC 797		12 25 24.2	+18 08 29	dE3,N	17.0	773 ± 8	9
VCC 810		12 25 33.6	+13 13 37	dE0,N	16.5	−340 ± 50	1
VCC 815		12 25 37.1	+13 08 36	dE2,N	16.1	−700 ± 50	1
VCC 817	IC 3313	12 25 37.7	+15 50 06	dE1	15.0	1086 ± 57	3
VCC 823		12 25 38.8	+12 18 49	dE0,N	15.7	1691 ± 33	2
VCC 833		12 25 44.4	+13 01 20	dE0,N	17.48	720 ± 50	1
VCC 846		12 25 50.3	+13 11 52	dE1,N	16.2	−730 ± 50	1
VCC 854		12 25 55.6	+12 46 11	dE8,N	17.3	684 ± 75	3
VCC 856	IC 3328	12 25 57.9	+10 03 14	dE1,N	14.42	972 ± 32	2
VCC 871		12 26 05.6	+12 33 34	dE,N	15.4	1636 ± 76	3
VCC 872		12 26 00.7	+12 51 40	dE0.N	17.0	1183 ± 50	3
VCC 882	NGC 4406B	12 26 15.6	+12 57 51	dE3,N	16.7	1101 ± 55	10
VCC 896		12 26 22.5	+12 47 00	dE3,N	17.8	2114 ± 63	3
VCC 916		12 26 33.3	+12 44 24	dE1,N	16.2	1115 ± 32	3
VCC 917	IC 3344	12 26 32.4	+13 34 43	dE6	14.8	1375 ± 66	2
VCC 928		12 26 39.6	+12 30 48	dE6,N	16.2	−254 ± 54	3
VCC 940	IC 3349	12 26 47.1	+12 27 15	dE1,N	14.78	1563 ± 57	9
VCC 951	IC 3358	12 26 54.4	+11 40 06	dE2p,N	14.23	2066 ± 21	2
VCC 953		12 26 54.6	+13 33 57	dE5?p,N	15.70	−629 ± 65	2
VCC 965	IC 3363	12 27 02.9	+12 33 37	dE7,N	15.40	790 ± 50	9
VCC 967		12 27 04.0	+12 51 54	dE4	18.7	1135 ± 51	3
VCC 977		12 27 11.1	+12 02 18	dE4,N	17.9	102 ± 45	3
VCC 990	IC 3369	12 27 17.1	+16 01 30	dE4,N	14.81	1727 ± 34	2
VCC 996		12 27 21.2	+13 06 36	dE5	18.4	−28 ± 32	3
VCC 1027......		12 27 38.0	+12 52 48	dE0,N	18.1	77 ± 46	3
VCC 1036......	NGC 4436	12 27 41.6	+12 18 59	dE6,N	14.03	1163 ± 50	2
VCC 1040......		12 27 44.5	+12 58 55	dE3,N	17.5	−143 ± 63	3
VCC 1042......		12 27 45.8	+12 52 19	dE4	18.6	−62 ± 13	3
VCC 1073......	IC 794	12 28 08.6	+12 05 36	dE3,N	14.23	1899 ± 19	2
VCC 1075......	IC 3383	12 28 10.7	+10 17 43	dE4,N	14.95	1844 ± 40	2
VCC 1087......	IC 3381	12 28 15.1	+11 47 23	dE3,N	14.42	645 ± 27	2
VCC 1104......	IC 3388	12 28 27.9	+12 49 24	dE5,N	15.31	1704 ± 31	2
VCC 1122......	IC 3393	12 28 41.7	+12 54 57	dE7,N	14.82	436 ± 29	2

TABLE 3—*Continued*

Name	Identification	R.A. (J2000.0)	Decl. (J2000.0)	Type[a]	Magnitude	v (km s^{-1})	Reference
VCC 1164......		12 29 07.8	+09 26 31	dE6,N	16.8	1040 ± 10	9
VCC 1173......		12 29 14.7	+12 58 42	dE5,N	16.06	2468 ± 68	8
VCC 1185......	M87DW07	12 29 23.4	+12 27 02	dE1,N	15.56	500 ± 50	1
VCC 1254......	NGC 4472DW08	12 30 05.3	+08 04 29	dE0,N	15.0	1350 ± 29	2
VCC 1261......	NGC 4482	12 30 10.4	+10 46 46	dE5,N	13.66	1850 ± 30	2
VCC 1308......	IC 3437	12 30 45.8	+11 20 34	dE6,N	15.1	1721 ± 45	2
VCC 1348......	IC 3443	12 31 15.7	+12 19 54	dE0p,N	15.64	1679 ± 39	1
VCC 1351......		12 31 17.5	+13 49 42	dE4	16.0	187 ± 48	3
VCC 1355......	*IC 3442	12 31 20.0	+14 06 53	dE2,N	14.31	1332 ± 63	11
VCC 1386......	IC 3457	12 31 51.3	+12 39 21	dE3,N	14.43	1426 ± 60	1
VCC 1407......	IC 3461	12 32 02.7	+11 53 25	dE2,N	14.82	919 ± 55	1
VCC 1420......	IC 3465	12 32 12.2	+12 03 43	dE4,N	16.2	1022 ± 87	2
VCC 1431......	IC 3470	12 32 32.4	+11 15 46	dE0,N	14.51	2025 ± 75	2
VCC 1453......	IC 3478	12 32 44.2	+14 11 46	dE2,N	14.34	1949 ± 26	2
VCC 1489......	IC 3490	12 33 13.8	+10 55 44	dE5,N	15.89	80 ± 50	2
VCC 1491......	*IC 3486	12 33 14.0	+12 51 28	dE2,N	14.8	903 ± 42	2
VCC 1514......		12 33 37.7	+07 52 16	dE7,N	15.1	538 ± 72	2
VCC 1539......		12 34 06.8	+12 44 30	dE0,N	15.4	1390 ± 50	1
VCC 1549......	IC 3510	12 34 14.7	+11 04 18	dE3,N	14.63	1357 ± 37	1
VCC 1567......	IC 3518	12 34 30.9	+09 37 28	dE5,N	14.64	1440 ± 55	2
VCC 1661......		12 36 24.0	+10 23 00	dE0,N	15.7	1400 ± 50	1
VCC 1669......		12 36 30.4	+13 38 16	dE6,N	16.2	600 ± 50	1
VCC 1713......		12 37 29.0	+04 45 02	dE	15.1	1655 ± 25	5
VCC 1743......	IC 3602	12 38 06.6	+10 05 01	dE6	15.1	1279 ± 51	1
VCC 1826......	IC 3633	12 40 11.2	+09 53 46	dE2,N	14.87	2033 ± 30	2
VCC 1828......	IC 3635	12 40 13.4	+12 52 29	dE2,N	14.9	1517 ± 57	2
VCC 1857......	IC 3647	12 40 53.2	+10 28 33	dE4,N?	14.33	634 ± 69	2
VCC 1861......	IC 3652	12 40 58.4	+11 11 03	dE0,N	14.37	683 ± 54	2
VCC 1870......		12 41 15.3	+11 17 55	dE6	15.8	1617 ± 27	3
VCC 1876......	IC 3658	12 41 20.4	+14 42 02	dE5,N	14.85	45 ± 49	2
VCC 1881......		12 41 29.5	+10 45 46	dE3;,N	16.2	138 ± 56	3
VCC 1886......		12 41 39.4	+12 14 52	dE5,N	14.87	1159 ± 65	2
VCC 1890......	IC 3665	12 41 46.3	+11 29 15	dE4p	14.84	1227 ± 57	2
VCC 1891......		12 41 48.9	+11 11 29	dE4,N	16.7	1016 ± 43	3
VCC 1897......	UGC 7857	12 41 54.2	+13 46 22	dE4,N	14.49	18 ± 60	2
VCC 1910......	IC 809	12 42 07.8	+11 45 16	dE1,N	14.17	206 ± 26	2
VCC 1919......		12 42 19.0	+10 34 04	dE0,N	17.0	1869 ± 54	3
VCC 1941......		12 42 50.0	+13 17 38	dE	18.0	1213	12
VCC 1947......		12:42 56.3	+03 40 35	dE2,N	14.56	944 ± 35	5
VCC 1948......		12 42 58.0	+10 40 55	dE3	15.1	1581 ± 22	3
VCC 1949......	NGC 4640	12 42 58.1	+12 17 10	dE6,N	14.19	2077 ± 75	9
VCC 1958......		12 43 10.0	+11 02 12	dE2,N	17.0	1049 ± 30	3
VCC 1971......		12 43 31.0	+11 02 50	dE3	16.6	1376 ± 34	3
VCC 2012......	IC 3727	12 45 05.7	+10 54 03	dE1,N	14.30	2230 ± 11	9
VCC 2019......	IC 3735	12 45 20.4	+13 41 33	dE4,N	14.55	1895 ± 44	2
VCC 2050......	IC 3779	12 47 20.7	+12 09 59	dE5,N	15.2	1367 ± 75	2
VCC 2062......		12 47 59.9	+10 58 33	dE	19.0	1146 ± 8	13

[a] Morphological types are from the estimates given by Binggeli et al. 1985.

REFERENCES.—(1) Binggeli et al. 1993, (2) Binggeli et al. 1985, (3) this paper, (4) Young & Currie 1995, (5) Grogin et al. 1998, (6) Duprie & Schneider 1996, (7) Zabludoff & Mulchaey 1998, (8) Drinkwater et al. 1996, (9) de Vaucouleurs et al. 1991, (10) Strauss et al. 1992, (11) Huchra et al. 1993, (12) Rubin, Waterman, & Kenney 1999, (13) Hoffman et al. 1996.

simple relaxed system with a Gaussian velocity distribution (see Figs. 4–8). Figure 7 shows the velocity of each Virgo galaxy, relative to the mean Virgo velocity of 1064 km s^{-1}, as a function of the absolute magnitude. The dashed lines show the escape velocity from the Virgo core computed from the mass profile of Giraud (1999). From Figure 7 we see no equipartition of energy, nor any obvious dynamical friction effects that would produce lower velocities for higher mass objects.

3.1.1. *Virgo Clouds: Galaxies Bound to the Cluster?*

Figure 3 shows the velocities of objects across the Virgo cluster. Triangles represent galaxies with velocities less than 1000 km s^{-1}, with larger symbols signifying larger velocity deviations from 1000 km s^{-1}. Circles are galaxies with velocities larger than 1000 km s^{-1}, with the largest circles signifying galaxies at $v > 2000$ km s^{-1}. Signatures of various "subclusters" or clouds can be seen from the different symbols. The spatial clustering in Figure 3 is, however,

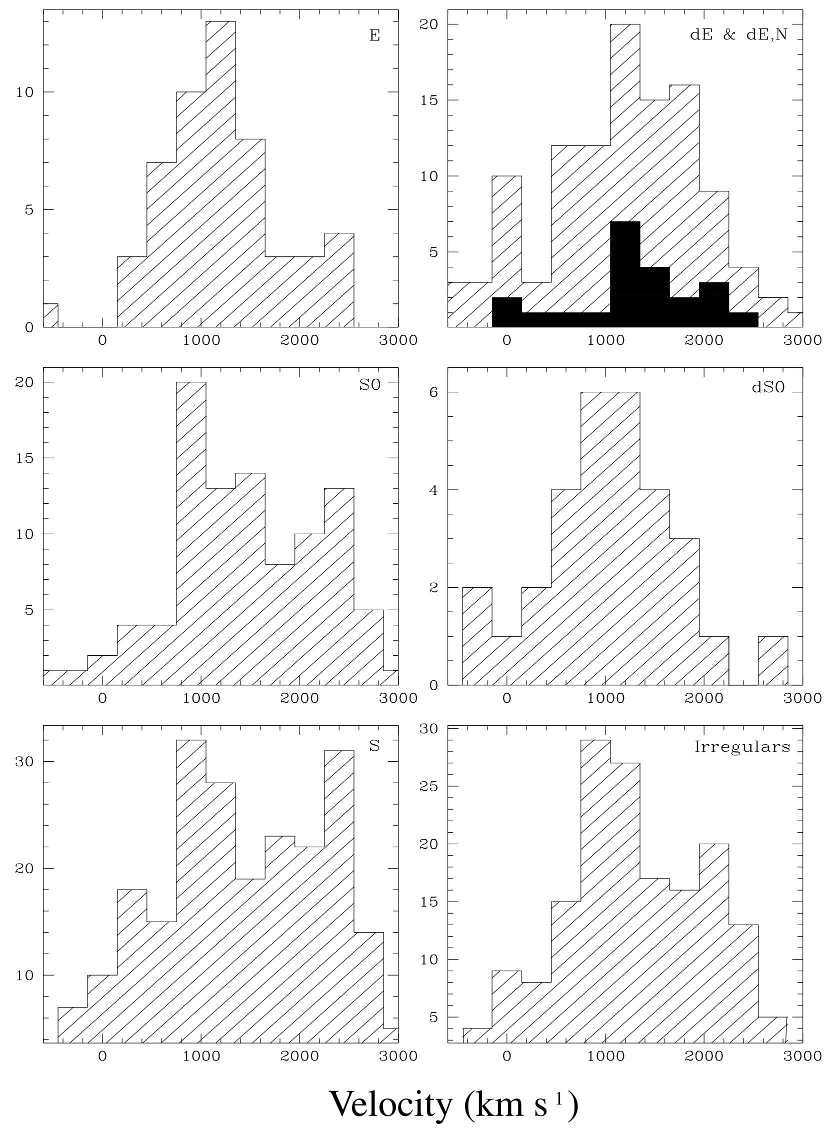

FIG. 4.—Velocity histograms of six galaxy populations contained in the entire Virgo sample. The solid part of the dE and dE,N histogram represents the nonnucleated dEs, while the shaded area is the combined dE and dE,Ns.

partially the result of selection biases introduced by spectroscopic sample selection.

There is evidence, however, for spatial clustering in Virgo, as is shown in Figure 6. SBB99 found that galaxy clustering correlates with the intensity of X-ray–emitting gas in Virgo. In the north, there is a subcluster with lower velocities associated with the Virgo cloud around M86. Likewise, we see velocity structures near M87 (the cross in Fig. 3) and the W cloud near (J2000) (α, δ) $\approx$ (12.35, 8.00).

The dEs also appear to clump slightly around the three major elliptical galaxies in Virgo: M87, M49, and M86. Within a degree of each of these galaxies the velocity dispersion of dETs is essentially the same as the dispersion of all Virgo dETs. For the five dETs within 0°.5 of M87, the dispersion is 428 km s^{-1} with a 14% chance of being random and an average velocity of 1097 km s^{-1}. The velocity of M87 is 1307 km s^{-1}, and thus there appears to be a strong clustering of a few dEs around it. The 18 dEs within 0°.5 of M86 (with $v = -244$ km s^{-1}) have an average velocity of 508 $\pm$ 812 km s^{-1}, which has only a 0.1% change of being random. M49, located at the southern part of the Virgo cluster, is spatially a separate system but has a similar velocity (997 km s^{-1}) to that of the Virgo core region. We see some evidence for dET association with this elliptical galaxy and its surrounding cloud. Within 0°.5 of M49 there are no dETs, but within 2° there are six dETs with a velocity of 1083 km s^{-1} and a low-velocity dispersion of 291 km s^{-1},

TABLE 4

MEAN AND σ FOR VIRGO "CORE" POPULATIONS

Class	Mean (km s^{-1})	σ (km s^{-1})	Median (km s^{-1})	N
E	1090 $\pm$ 73	462	1095	40
S0	1164 $\pm$ 86	647	1115	56
dE	1146 $\pm$ 150	636	1220	18
dE,N	1033 $\pm$ 84	747	1159	79
dET	1054 $\pm$ 73	726	1159	97
dS0	960 $\pm$ 116	612	895	28
Irr	1054 $\pm$ 81	727	1100	81
S	1056 $\pm$ 71	776	1037	119
Virgo	1064 $\pm$ 34	705	1100	429

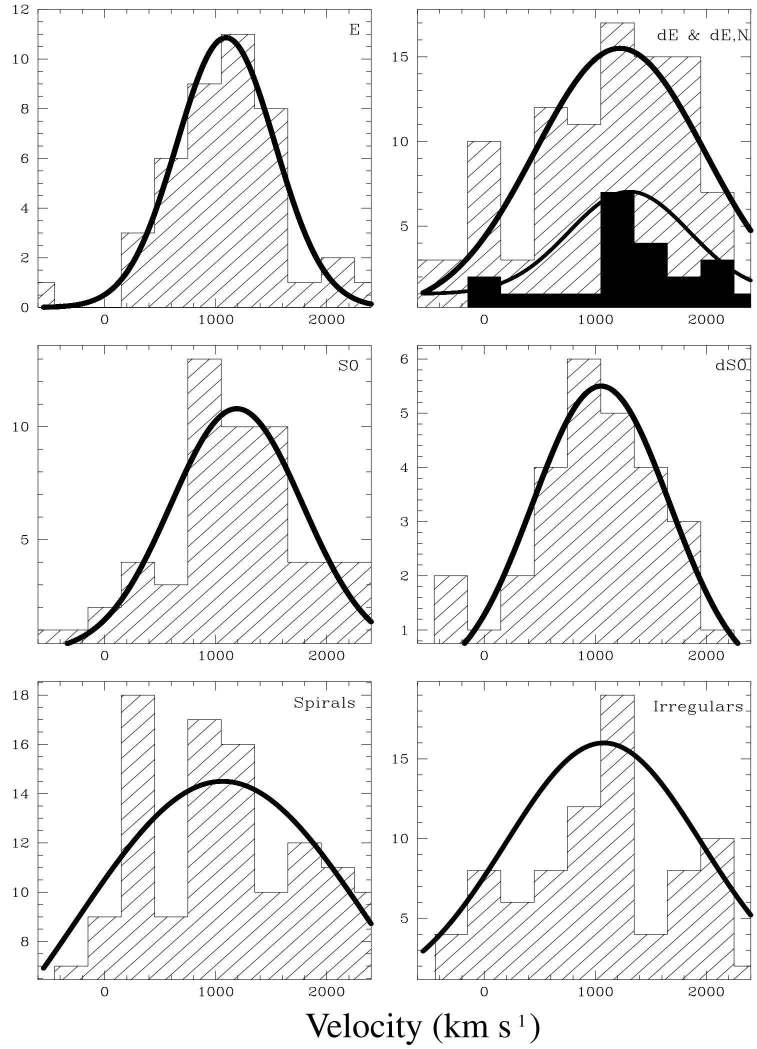

FIG. 5.—Velocity histograms for the Virgo "core" population, with fitted Gaussian profiles. The galaxies here are the subsample of galaxies in Fig. 4 that are within 6° from the dynamical center of Virgo (see text) and whose radial velocities are less than 2400 km s^{-1}. The solid part of the dET histogram represents the pure dEs.

with a 2% change of being random. This dispersion remains low (473 km s^{-1}) for all dETs within 3° of M49. This has been known for some time for all galaxies in the M49 region (Binggeli et al. 1987). We conclude, in agreement with Ferguson (1992), that there is some evidence for bound dE companions to giant galaxies in Virgo, but it is only a statistically significant effect for M86. As is suggested from their spatial positions, most dEs are distributed in the general gravitational potential of Virgo and are not companions of larger galaxies.

To determine if the velocity and projected locations of the various galaxy populations are statistically distinct, we perform Kolmogorov-Smirnov (K-S) tests on the positions and velocities of each individual core population against each of the other individual core populations. We do not perform these tests for the total galaxy populations, but only the core ones, to avoid biases from other Virgo galaxy clouds. These are two-sided K-S tests that compare the distributions of velocities and positions of galaxies in different populations with each other (e.g., Press et al. 1992). Since K-S tests are based on statistics of two vectors, the positional test is limited to the projected radial distance from the center of the cluster. These tests are also somewhat constrained since if galaxies are in equilibrium their spatial positions and velocities should reflect the underlying mass distribution of the cluster. As such the interpretation of a lack of a correlation between two populations is not straightforward. On the other hand, if two populations were accreted into Virgo at the same time, then we might expect their orbital and spatial positions to be correlated.

The results of these tests are shown in Tables 5 and 6. Unfortunately, the results are largely inconclusive, showing no statistically significant correlation between any two populations, but they are instructive in several cases. We discuss individual K-S tests for each Virgo galaxy population in § 3.3.

3.2. *Accretion and Orbit Signatures*

Figure 9 shows pie diagrams of slices through the total Virgo sample in both right ascension and declination. These

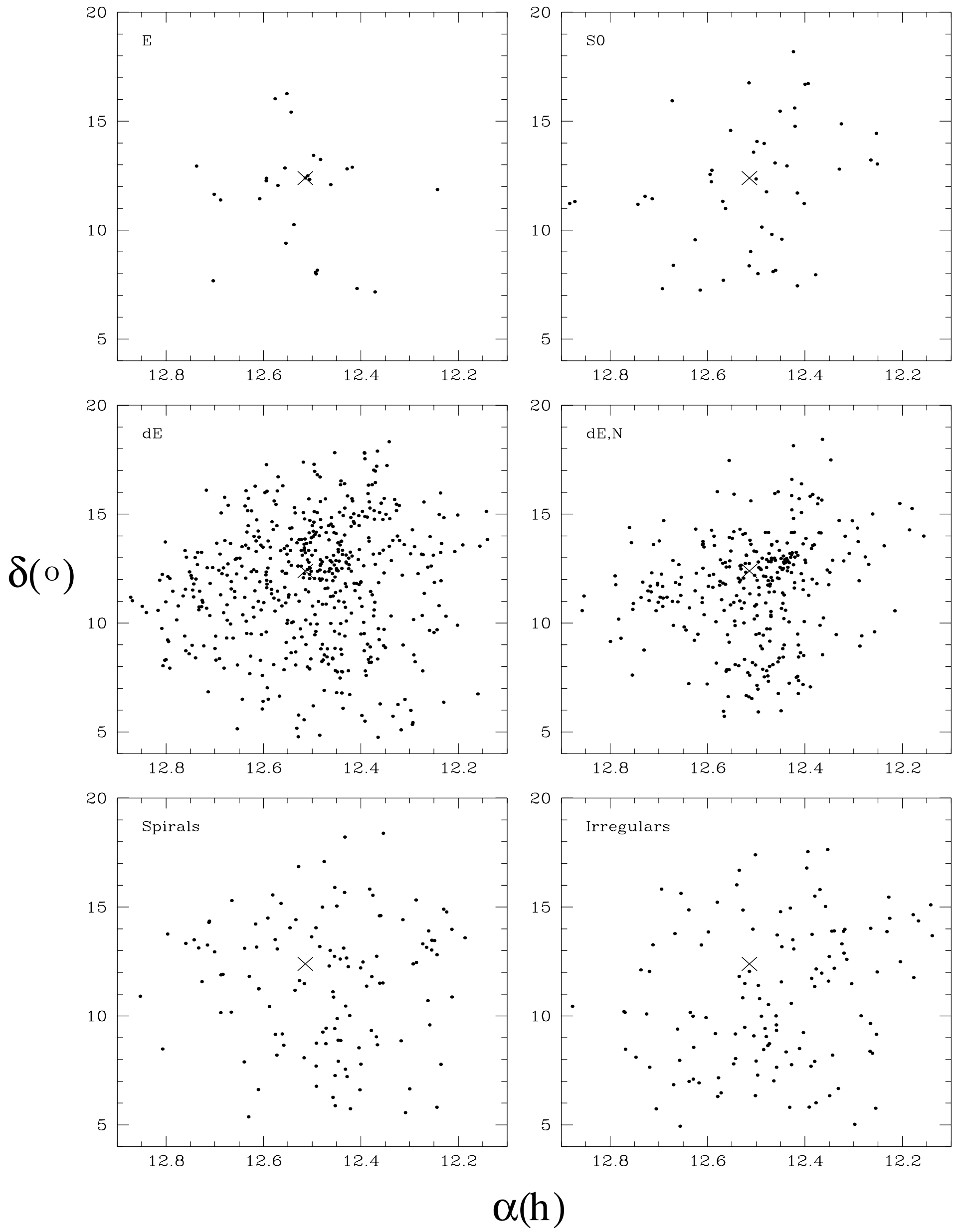

FIG. 6.—Positional plots of the various Virgo populations. These contain all galaxies considered by Binggeli et al. (1985) to be within Virgo based on velocity and/or morphological information. The cross represents the location of M87.

figures have several features that illustrate the dynamical state of the Virgo cluster. The first is the clear "finger of god" signature of the virialized Virgo core. The population here is a mixture of all morphological types.

Also in these figures are clear indications of galaxies still in the process of accreting into the Virgo core. These produce shell-like "infall ring" regions, perpendicular to our line of sight in a pie diagram (Praton & Schneider 1994).

TABLE 5

K-S TEST RESULTS FOR RADIAL VELOCITIES

Class	E	S0	dE	dE,N	dET	dS0	Irr	Spirals
E..........	100	38.7	60.9	39.1	36.8	29.7	36.8	9.6
S0.........	38.7	100	62.0	34.7	48.0	26.7	59.1	19.7
dE	60.9	62.0	100	66.1	...	46.0	53.5	35.4
dE,N......	39.1	34.7	66.1	100	...	70.0	85.4	67.3
dET.......	36.8	48.0	...	...	100	52.0	81.4	48.7
dS0	29.7	26.7	46.0	70.0	52.0	100	73.1	45.0
Irr.........	36.8	59.1	53.5	85.4	81.4	73.1	100	91.5
S	9.6	19.7	35.4	67.3	48.7	45.0	91.5	100

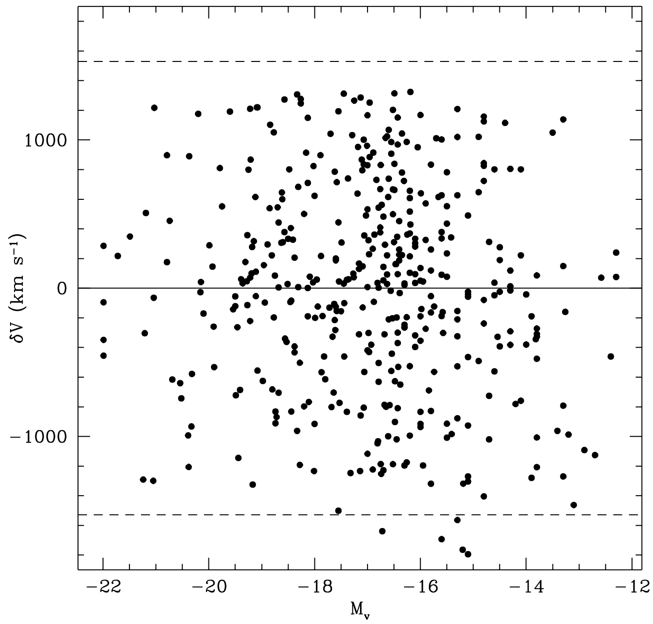

FIG. 7.—Relative velocities of Virgo galaxies plotted as a function of their absolute magnitudes assuming a Virgo distance modulus of $(m - M) = 31.3$. From this plot there is no sign of mass-velocity segregation or energy equipartition in Virgo. The dashed lines represent the escape velocity of Virgo.

In Figure 9 there are also several clumpy areas that contain galaxies, sometimes very close to the "finger of god" feature. By far the most common galaxy to deviate from the "finger" are the spirals, which define these clumpy regions. The dETs (*open circles*) tend to follow both the spirals (*crosses*) and ellipticals (*black squares*); outer associations are dominated by spirals and dwarf ellipticals, but with a very high spiral/dET ratio.

While velocities of spirals and ellipticals in Virgo are almost all known, only a very small fraction of dET velocities have been measured. Of these, most are for dETs in the densest regions, and mainly for the more easily observed dE,N types. It is therefore possible that dETs populate all regions of this diagram, especially in the outer associations dominated by later-type galaxies. Furthermore, velocity dispersions of various Virgo galaxies as a function of distance from the cluster core (Fig. 10) indicate that dEs are on complex orbits. This is also true for the spirals, S0s, dS0s, and irregulars, indicating that these systems have a mix of orbits including highly elliptical or radial ones.

3.3. *Velocity Distributions*

If some galaxies in Virgo originate from an accreted component that underwent interactions with other cluster members, and if the velocities reflect only the gravitational potential well of Virgo at time of infall, then the various velocity dispersions of accreted populations should be somewhere between that of the old giant E component, assuming they trace the early potential (see § 3.3.1), and currently infalling spiral and irregular galaxies. The evolution of the distribution of velocities of Virgo galaxy populations and their dispersions can be predicted by using reasonable assumptions about their total lifetimes in the cluster. This can be done by investigating the effects of two-body relaxation, equipartition of energy, and dynamical friction.

To test these ideas we produced velocity histograms (Figs. 4 and 5) and statistical data (Tables 5 and 6) on the

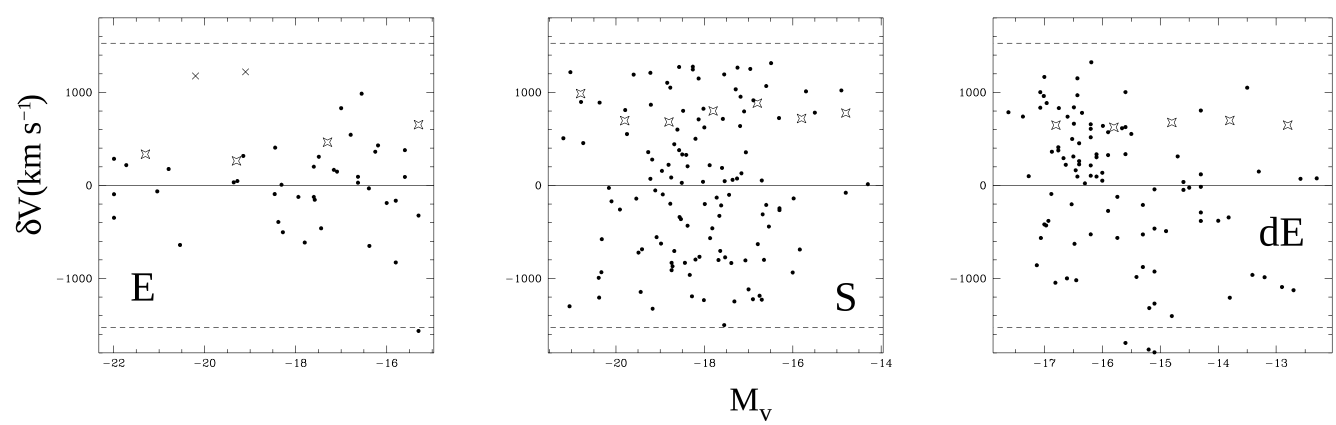

FIG. 8.—Elliptical, spiral, and dET velocities as a function of magnitude. The open stars represent the velocity dispersion as a function of magnitude. The two upper crosses in the elliptical galaxy plot are two galaxies in our sample that are likely not part of the Virgo cluster proper or true ellipticals (see text).

TABLE 6

K-S TEST RESULTS FOR PROJECTED RADIAL POSITIONS

Class	E	S0	dE	dE,N	dET	dS0	Irr	Spirals
E	100	26	11	64	23	32	0	2
S0	26	100	68	5	30	45	15	62
dE	11	68	100	0	...	90	0	3
dE,N......	64	5	0	100	...	17	0	0
dET	23	30	...	...	100	62	0	0
dS0	32	45	90	17	62	100	2	25
Irr	0	15	0	0	0	2	100	12
S	2	62	3	0	0	25	12	100

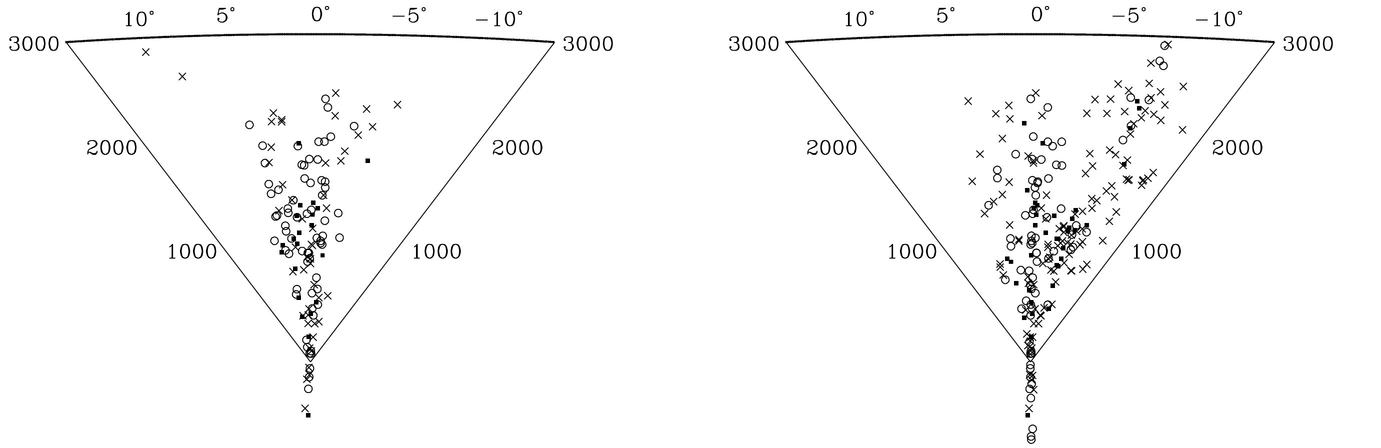

FIG. 9.—Declination and right ascension velocity slices through the core of Virgo showing the "finger of god" signature and infall ring patterns. The spirals are crosses, ellipticals are black squares, and dwarf ellipticals open circles. Several other clumpy regions can be seen in this diagram, most particularly at (−3°, 1000 km s^{-1}) and (−5°, 2000 km s^{-1}).

total (Fig. 4) and core (Fig. 5) Virgo galaxy populations, including giant ellipticals (E), spirals (Sa–Sd), dwarf ellipticals (dE) nucleated dwarf ellipticals (dE,N), lenticulars (S0), dwarf lenticulars (dS0), and irregulars (dIrr, I, Sm, BCD).

We fit Gaussian distributions to all of the core histograms (Fig. 5) by using the Levenberg-Marquardt (LM) algorithm (Marquardt 1963). We use the results of these fits to test for kinematic characteristics of infalling versus bound galaxy populations. In particular, a Gaussian form is expected for a virialized population. Thus finding how well a Gaussian can fit a velocity distribution is one method for determining if a population might be relaxed. The Levenberg-Marquardt method uses a nonlinear least-squares routine to fit the number of galaxies (N) as a function of velocity (v) in the form:

$$N = A + B \times v + \Sigma\left\{C \times \exp\left[-2.7 \times \left(\frac{(v - \text{center})}{\text{FWHM}}\right)^2\right]\right\}, \quad (1)$$

where A and B are constants and always fit to zero, and C is the amplitude of the Gaussian, while "center" and "FWHM" are the center and full width at half maximum for the fitted Gaussians. This summation is over the total number of Gaussians needed to fit the distributions. For cases where either one or two Gaussian components could be fitted, we present in Figure 5 only single Gaussians. The centers of the peaks are also fitted by the LM algorithm, and not chosen a priori by us.

The different velocity distributions for galaxy populations in the total Virgo sample can be seen in Figure 4. The ellipticals, spirals, lenticulars, and irregulars have bimodal distributions. The second peak located near 2500 km s^{-1} is largely the result of projected clouds that are probably falling into the main cluster (Virgo A in Binggeli et al. [1987] and Virgo I in de Vaucouleurs & de Vaucouleurs [1973]). Interestingly, there is little evidence of this second 2500 km s^{-1} peak in the dET and dS0 populations. This is an indication that nucleated dwarf ellipticals are abundant only in the well-defined rich Virgo cluster proper, located near a velocity of 1000 km s^{-1}. The nucleated dwarf ellipticals and dS0 population are associated with the dynamical Virgo core or Virgo A cloud at $V = 1064$ km s^{-1}, although significant substructure is evident.

3.3.1. *Ellipticals*

The radial velocity distribution of ellipticals changes slightly between the total Virgo area and the Virgo core (Figs. 4 and 5), with a 75% probably of association from a K-S test. The secondary distribution centered at 2500 km s^{-1} is almost completely absent in the Virgo core population, and the radial velocity distribution of the core ellipticals can be fitted as a single Gaussian distribution with the best-fit $\chi^2 = 1.66$, peak at 1093 km s^{-1}, and a velocity dispersion $\sigma = 462$ km s^{-1}.

Despite this, even in the core population, there are ellipticals with highly deviant velocities for their magnitudes (Fig. 8). One galaxy at 2284 km s^{-1}, NGC 4168, is uncertain as a member of the Virgo cluster proper (VCC) and has an uncertain classification owing to its probable low mass (Ho et al. 1997). Another high relative radial velocity galaxy is NGC 4473 with $v = 2240$ km s^{-1}. It is also doubtful that this galaxy is a proper member of the Virgo core or even an elliptical. It contains disky isophotes, evidence of dust (Michard & Marchal 1994; van den Bosch et al. 1994) and its properties do not fit elliptical galaxy scaling relations (Davies et al. 1983).

Excluding these two galaxies from the elliptical population we see a slight, but statistically insignificant, signature of equipartition of energy or effects of dynamical friction. The giant E galaxies appear by eye to have a decreasing dispersion with increasing mass, a possible signature of a process that has led to the giant ellipticals being more dynamically bound in the cluster. To test if this result is statistically significant, we carry out a Monte Carlo simulation of the velocities and magnitudes for these ellipticals. We characterize the mass-velocity segregation by measuring the difference between the velocity dispersion for the bright ($M_V < -19$) and faint ($M_V > -19$) ellipticals. The velocity dispersions of these two components are 299 km s^{-1} and 509 km s^1, respectively, a 210 km s^{-1} difference. Using Monte Carlo techniques, we find a 2% chance that this difference is random and that the observed difference is a 2.3 σ event. It is therefore likely that this magnitude-velocity difference is due to chance, and not a real physical

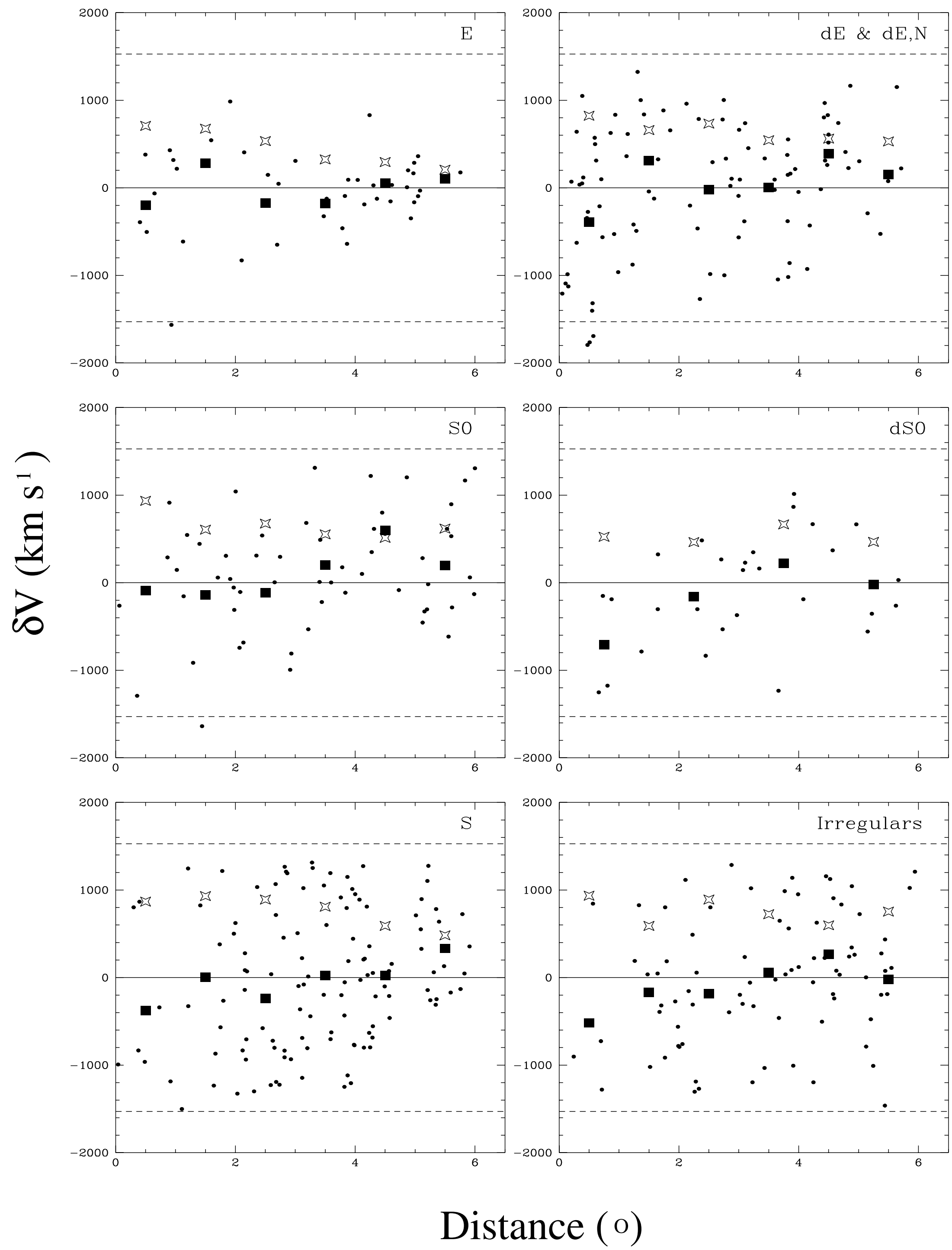

FIG. 10.—Radial velocities of the Virgo galaxy populations plotted as a function of projected distance from the center of Virgo. The high velocity dispersions (*open stars*) at the center of Virgo indicate that galaxies in Virgo are on radial or highly elliptical orbits. The black squares represent the average velocity at each distance.

effect. This signature is removed completely if we include the two rejected ellipticals.

The ellipticals in the Virgo core region have the lowest total velocity dispersion $\sigma = 462$ km s^{-1} of the major cluster populations, a Gaussian velocity distribution (Fig. 5), and a centrally concentrated spatial distribution (Fig. 6). These all suggest that ellipticals are the oldest and most relaxed component in Virgo. Distances derived from surface brightness fluctuations also suggest that most of the ellipticals in Virgo are gravitationally bound to the cluster (Neilsen & Tsvetanov 2000). Figure 10 shows the steadily decreasing value of the projected velocity dispersion as a function of projected distance from the dynamical center of Virgo for the elliptical population. Virgo ellipticals appear to be more dynamically relaxed in comparison to other populations. These effects are also seen for relaxed populations in N-body simulations of structure formation (e.g., Crone, Evrard, & Richstone 1994; Thomas et al. 1998).

3.3.2. *Lenticulars* (*S0s*)

Depending on their nature, cluster lenticulars (S0s) may provide a critical clue to the evolution of galaxies in dense extragalactic environments (Dressler 1984). The major question to answer is whether or not this population has an origin more similar to the ellipticals or to the spirals. Being a "transition-type," the lenticulars have properties of both ellipticals (old stellar populations, symmetric structure) and spirals (outer disks).

The kinematics of the S0 population in Virgo clearly differ from those of the ellipticals. The velocity dispersion of the S0s is 647 km s^{-1}, almost 200 km s^{-1} higher than that of the elliptical population, and similar to that of the dET population. Based on their radial velocities and positions, there is a 62%–68% probability that the dEs originate from the same population as the S0s, although there is a lower 5%–39% probability for a velocity association with the dE,Ns. The S0s are clearly more extended spatially than are the ellipticals (Fig. 6) and again resemble the spirals and dEs in this aspect. Their velocity distribution also contains a low-velocity component near 300 km s^{-1} that is also seen in the dET, spiral and irregular populations. The overall velocity distribution for S0s is not fitted very well by a Gaussian. The clumpy distribution of S0 velocities indicates that these galaxies are not a relaxed Virgo component.

Based on this we conclude that S0s are *not associated* with ellipticals, but formed later, potentially by a process similar to that by which the dEs form (Mao & Mo 1998; Moore et al. 1999). This is consistent with observations of higher redshift $z \sim 0.5$ clusters, where the S0 fraction is as much as three times lower than that seen in nearby clusters (Dressler et al. 1997), while the fraction of ellipticals in clusters is found to be the same at $z < 1$ (Dressler et al. 1997). High-resolution N-body simulations of cluster formation based on a CDM scenario also show that the properties of S0s cannot be reproduced from major mergers, while those of elliptical galaxies can (Okamoto & Nagashima 2001), suggesting that S0s formed later.

3.3.3. *Spirals and Irregulars*

The spiral galaxy population has a wide non-Gaussian velocity distribution with a total core velocity dispersion $\sigma \sim 776$ km s^{-1}, over 300 km s^{-1} higher than that of the ellipticals (Table 4). The multipeaked and broad velocity histogram (Figs. 4 and 5) can be interpreted as a result of spiral-rich groups infalling into the cluster. Huchra (1985) characterized the velocity structure of the Virgo spirals as "flat-top." However, our lower errors allow finer binning, and there appear to be three components centered near 300 km s^{-1}, 1100 km s^{-1} and 1900 km s^{-1}. Similar peaks are seen in the dET, S0, and irregular populations. For an infall model, the high-velocity components are spirals falling into Virgo on the side nearest the Local Group, while the low-velocity components are spirals falling toward us on the opposite side.

Further evidence that some Virgo spirals were recently accreted is shown by a pattern of lessening gas depletion within spirals at greater projected radii from the central cluster core, where the hot dense ICM could removed gas by ram-pressure (e.g., Haynes & Giovanelli 1986; Cayatte et al. 1990; Solanes et al. 2001). Spirals far from the core are mainly falling into the cluster, while those in the inner part of Virgo have begun to go through the core, and as a result of gas stripping by the ICM, are depleted of gas. Distances to Virgo galaxies derived from the Tully-Fisher relation also reveals the expected infall velocity pattern: galaxies with blue shifts relative to the cluster are furthest away (Gavazzi et al. 1999).

The spirals in Virgo are statistically similar in velocity space only to the irregulars (Table 5). Is it possible that irregulars were once satellites of present day Virgo spirals? During infall companions of spirals will be separated by tidal forces. The potential of Virgo will induce, for pure linear motion and linear arrangement between, for example, a spiral of mass M_{sp} and a companion, a maximum radial differential acceleration of

$$a_{clu} = GM_{clu}\left\{\frac{1}{r^2} - \frac{1}{[(r+R)^2]}\right\}. \quad (2)$$

The spiral and its companion will become dislodged when $a_{clu} > GM_{sp}/R^2$. In these equations, R is the distance between the infalling spiral and its companion, r is the distance from the leading edge of the group to the center of the cluster, M_{clu} and M_{sp} are the masses of the cluster and infalling spiral, and G is the gravitational constant. This formula changes somewhat in a nonradial situation, since equation (2) is only valid for a radial force. If we take the mass of Virgo as $10^{14}\ M_\odot$, concentrated within r, and an infalling spiral galaxy with mass 10^{10}, then a galaxy separated by 0.5 Mpc from the host spiral will become dislodged within 2.5 Mpc of the cluster center. We can generalize this by using radial tides on an infalling galaxy of mass M_{gal} and a companion that will become dislodged when $RGM_{clu}/r^3 = GM_{gal}/R^2$, which occurs at $r = 10$ Mpc.

The irregulars[4] in, or projected against, the core have characteristics very similar to the spirals and in some ways also to the dwarf ellipticals. The low- and high-velocity components are present in the irregular population (Fig. 5), and the spatial distribution is very similar to that of the spirals (Fig. 6). There is also a 92% probability that the irregulars originated from the same velocity population as the spirals, as shown by K-S tests (Table 5).

From the triple-peaked velocity distribution and the high-velocity dispersion of 727 km s^{-1}, similar to that which we see for the spirals, it seems likely that the irregular population is infalling into the cluster along with the spirals (e.g., Gallagher & Hunter 1989). Their high gas content and star formation rates indicate these objects have not yet crossed the cluster core, where their extended gas will be rapidly stripped by the intracluster medium (see Lee et al. 2000; Mori & Burkert 2000).

3.3.4. *Dwarf Ellipticals*

The overall dET population has a velocity distribution that is similar to that of the spirals but not to that of the ellipticals, with a velocity dispersion of 726 km s^{-1}, compared to the value of 776 km s^{-1} for the spirals, and 462 km s^{-1} for the ellipticals. This general trend has been suspected for some time and found by previous studies (e.g., Bothun & Mould 1988), but also has been disputed on the basis of

[4] It is worth repeating for clarification that our irregular population includes Magellanic Spirals (Sm), as well as the classical dwarf irregulars and blue compact dwarfs. Any comparisons to other studies should keep this in mind.

smaller samples than the one used here (Binggeli et al. 1987). The projected spatial distribution of the dETs, like that of the spirals, does not show as significant a decline in radius as does that of the ellipticals. To which of these two major populations are the dETs similar? The velocity distributions and dispersions of both dETs and pure dEs (Figures 4 and 5) resemble more the spirals rather than the ellipticals.

The distribution of dET velocities is not fitted by a single Gaussian, another indication of dynamical evolution, youth, and/or substructure. If Virgo dEs were in equipartition with the giant ellipticals we would see evidence for mass-position segregation. In this case, the dEs would have a more extended spatial distribution and a larger velocity dispersion than what is observed (§ 4.1.1). In fact, many dEs are in the richest part of Virgo, with fewer found in the lower density areas (Fig. 6). Possibly some mass-position segregation is occurring, since the dEs are more spread out than the giant Es, but this is only a slight effect that could also be accounted for by dEs originating from accreted components not on radial orbits. The velocity distribution of the dEs is also clumpy, including evidence for a low-velocity peak (Fig. 5). From these data, we conclude that the dETs taken as a single population are less dynamically evolved than the Virgo cluster core E populations and are not relaxed. To further test this will require knowing the three-dimensional spatial distributions and velocity dispersion profiles of Virgo galaxies.

4. DYNAMICAL MODELS

Modeling the dynamical evolution of galaxies in Virgo is critical for understanding these various kinematic characteristics and how they evolve. In this section, we investigate various ways the velocity distributions of galaxy populations can change over time. This includes determining what the velocity distribution would be if all galaxies have been in the cluster since its initial formation. Based on these calculations we conclude, consistent with our observational data, that the elliptical population is the oldest, and only relaxed subcomponent of the cluster, while all the remaining populations have characteristics of later infall.

4.1. *Virialization and Relaxation*

The time for a galaxy in a cluster to relax can be approximated to an order of magnitude in several ways. One way is to use the two-body relaxation time (Chandrasekhar 1942; Spitzer & Hart 1971; Spitzer 1987). For a self-gravitating population of identical mass bodies, the two-body relaxation time t_r, defined as the time for a galaxy's orbit to become deflected by 1 radian, is given by

$$t_r = \sigma^3/(4\pi G^2 m_g^2\, n \ln \Lambda) \approx \frac{0.06N}{\ln(0.15N)} \times t_d \,, \qquad (3)$$

where σ is the velocity of the galaxy, m_g is the mass of the galaxy, n is the number density of cluster galaxies, Λ is the ratio of maximum to minimum impact parameters, N is the number of particles in the system, and t_d is the cluster crossing time.

To compute the total relaxation time for the Virgo elliptical population we assume that early in Virgo's history only the ellipticals existed. Assuming a primordial average elliptical mass of $10^{12}\ M_\odot$, an initial number density ~ 20 galaxy/Mpc^3, and a velocity dispersion of ~ 460 km s^{-1} (Table 2) gives a relaxation time of ~ 1.5 Gyr. The time for a system to completely relax is about $10 \times t_r$; thus it would take ~ 15 Gyr for the elliptical population to complete this process. This is approximately a Hubble time, and thus it is unlikely that relaxation has completely occurred.

The relaxation of the Es is however consistent with observations of galaxy populations in ($z \sim 0.5$) clusters where the "core" ellipticals seem to be well in place (Dressler et al. 1997). Furthermore, the star formation history of moderate redshift clusters suggest that the stellar populations of ellipticals are mostly formed by $z \sim 3$ (Ellis et al. 1997). This formation must occur early to account for the mass-metallicity relationship found in nearby cluster ellipticals (Kauffmann 1996).

This also agrees with results from numerical cold dark matter models that show the first objects to relax in clusters are large elliptical galaxies (Diaferio et al. 2001). Simulations of cluster formation also indicate that the first galaxies formed in clusters should now be preferentially at the center (White & Springel 2000; Governato et al. 2001). The ellipticals are consistent with being these objects since they are the most centrally concentrated population in Virgo.

For a dET population, similar to the present day density of several thousand dETs in a volume of a few Mpc^3, the time for relaxation is greater than 10^{13} yr, assuming all the Virgo mass then was contained in dEs. Thus relaxation is not likely to have occurred for any dETs, old or young.

4.1.1. *Energy Equipartition*

We can crudely estimate features of dEs if they have achieved energy equipartition with the giant ellipticals. In this scenario the average energies of the elliptical and dwarf ellipticals should be the same. This would require that the average velocity of the dET population be $(M_{\rm E}/M_{\rm dE})^{-1/2} \times V_{\rm E}$, where all quantities are averages. Taking the average mass of a Virgo elliptical and dwarf elliptical as 10^{12} and $10^8\ M_\odot$ respectively, and the observed velocity dispersion of 462 km s^{-1} for the ellipticals, the average velocity of the dEs should be $\sim 46 \times 10^3$ km s^{-1}. This velocity is much larger than the observed 726 km s^{-1} and is larger than the Virgo escape velocity. Dwarfs therefore would be escaping the cluster, and at the very least would have a very large velocity dispersion. We should also begin to see some mass segregation, with significant numbers of dETs in the outer parts of the cluster. Most dETs are, however, in the core region of Virgo, although with a large dispersion in distances (Young & Currie 1995; although see Binggeli & Jerjen 1998).

The timescale for energy equipartition to occur is given by (e.g., Bertin 2000, eq. 7.10),

$$t_{\rm eq} = \frac{m_f}{m_g} \times t_r \,, \qquad (4)$$

where t_r is the relaxation time (eq. [3]) and m_f is the mass of field particles. For the giant Es, $t_{\rm eq} \approx t_r = 1.5$ Gyr, although for dwarf ellipticals to reach equipartition with ellipticals $t_{\rm eq} > 10^3 \times t_r \sim 10^7$ Gyr. Based on this approximation the dETs and the other Virgo populations cannot be in equipartition of energy with the ellipticals. This is verified by our observations (Fig. 8) that shows no signs of equipartition in the dET or spiral population. However, the giant Es can be in equipartition with each other if we assume that the Es were the first and only galaxies in the cluster several Gyrs ago, and all additional galaxies were accreted adiabatically.

Any new dETs introduced into the cluster, as well as any old dETs, should show no signs of energy equipartition or full relaxation. Lacking these signatures therefore does not prove that Virgo dEs are a young cluster population.

4.2. *The Evolution of Velocity Structures and Evidence for Infall*

To understand how any new galaxy population introduced into Virgo will kinematically evolve, we consider the case of galaxies undergoing spherical accretion into a cluster at the turnaround radius, where the velocity of infall just cancels the expansion rate of the universe (Peebles 1980).

In the special case where the density perturbation associated with a galaxy cluster has a constant density within the turnaround radius R_T, we can write the mass within any radius r, where $r < R_T$ as $M(<r) = (4/3)\pi r^3 \rho$. The infall velocity of a galaxy joining a cluster with mass M, and turnaround radius R_T scales as $v^2 \sim \rho \times R_0^2 \sim M/R_T$. Thus, depending on the form of M/R_T, clusters with higher masses will contain accreted galaxies with higher radial velocities. This can generalized in the following way (e.g., Gott & Rees 1975). When the initial density enhancements in the universe can be represented by a power law after recombination, then

$$\frac{\delta\rho(t_0)}{\rho(t_0)} = \left(\frac{M}{M_0}\right)^{-1/2-n/6} , \quad (5)$$

where $n \geq -3$ for hierarchical clustering. For a universe with $\Omega = 1$, the mass and size, R_T, of assembled areas are related by

$$\frac{R_T}{R_0} = \left(\frac{M}{M_0}\right)^{5/6+n/6} . \quad (6)$$

Unless M/R_T remains static, or decreases, which requires $n \leq 1$, then galaxies accreted at later times when the cluster mass is higher, will have higher M/R_T ratios, and thus higher observed velocities, than when the cluster contained less mass. This is consistent with spirals and irregulars being the most recently accreted component since they have the highest velocity dispersions. The rate of shell infall increases with higher Ω_M, and for $\Omega_M = 1$ *all* shells eventually fall into the cluster. The current Virgo mass within a radius of 800 kpc is 1.8–3.3 $\times 10^{14}$ $M_\odot$, based on fits to mass profiles (Girard 1999) while SBB99 find a somewhat lower value. In the past Virgo likely contained a lower total mass, and any galaxies accreted then will have lower observed velocities than those captured recently.

Dynamical friction is also an important aspect to consider. We can compute the effective timescale for dynamical friction, in terms of the initial radius r_i, velocity V and mass M, assuming a static potential, as (Binney & Tremaine 1987)

$$t_{\rm fr} = \frac{264\ {\rm Gyrs}}{\ln\Lambda}\left(\frac{r_i}{2\ {\rm kpc}}\right)^2\left(\frac{V}{250\ {\rm km\ s^{-1}}}\right)\left(\frac{10^6\ M_\odot}{M}\right) . \quad (7)$$

For the ellipticals, $t_{\rm fr} \sim 3$ Gyr. This is short enough for dynamical friction to have an effect on the kinematic structure. This is especially true if ellipticals have existed in clusters for many Gyrs, as is suggested by observations (e.g., Ellis et al. 1997) and theory (Kauffmann 1996). For all other lower mass populations, including the dEs, dynamical friction is not an efficient process with $t_{\rm fr} \sim 10^3$–10^4 Gyrs.

We conclude from this argument, and the previous calculations in § 4.1, that velocities of low-mass ($<10^{10}$ $M_\odot$) accreted galaxies, and hence their velocity dispersions, should not change very much over a Hubble time as a result of dynamical friction, relaxation, or energy equipartition. If dEs are a new population that resulted from infall in the last several Gyr, then they should retain many of their original orbital characteristics. Two possibilities then exist for explaining a separation between giant ellipticals and the dEs. The ellipticals and dEs could have formed together and later the distribution of ellipticals modified to become more centrally concentrated due to dynamical evolution. Alternatively, the properties of the dEs may reflect later infall into the cluster.

We can use the fact that the ellipticals are relaxed while the other populations should retain their original orbital features to argue that most spirals and irregulars have recently been accreted, while the dET and S0 populations primarily originated from galaxies that fell in after the cluster core formed. For a virialized population the kinetic (T) and gravitational potential energy (U) should be related by $|T| = 1/2|U|$, while for an accreted population $U + T = 0$ and thus $|T| = |U|$. Assuming that on average the potential of a population that fell into Virgo is equal to the potential of a virialized population, we can relate the velocity dispersions of a virialized and infalling population, assuming isotropic orbits, as (see also Colless & Dunn 1996) $\sigma_{\rm infall} = \sqrt{2} \times \sigma_{\rm vir} = 1.41 \times \sigma_{\rm vir}$. For the Virgo populations the ratios of $\sigma_{\rm pop}/\sigma_{\rm E}$, where pop is any one of dEs, S0s, irregulars, or spirals, are $\sigma_{\rm dET}/\sigma_{\rm E} = 1.57$ or 1.51 if we include dS0s, $\sigma_{\rm S0}/\sigma_{\rm E} = 1.4$, $\sigma_{\rm Irr}/\sigma_{\rm E} = 1.57$, $\sigma_{\rm Spiral}/\sigma_{\rm E} = 1.65$. These values are all very close to that expected for the ratio between infalling and virialized populations, and are not obviously accounted for by the dynamical evolution models. We therefore favor the delayed infall model for the source of cluster dEs. If infall is occurring, orbital characteristics should also correlate with galaxy types; for example, star-forming galaxies should have unique orbital properties (Mahdavi et al. 1999; Balogh, Navarro, & Morris 2000), including large velocity dispersions which we see (Fig. 10).

4.3. *High-Speed Interactions*

Although neither dynamical friction nor relaxation induce major effects on the evolution of kinematics of low-mass cluster galaxy, high-speed or impulse interactions are potentially an important method for altering the internal properties of infalling galaxies. The interactions between galaxies in Virgo, with a total velocity dispersion of ~ 700 km s^{-1}, are nearly all at high-speed, at relative velocities much higher than individual internal galaxy velocity dispersions. Thus, it is instructive to investigate how these interactions can affect the properties of cluster galaxies. As we show here, high-speed interactions, while important, are rather inefficient at *destroying* low-mass galaxies, but are likely to significantly *modify* their structures.

We can approximate the strengths of high-speed interactions by using the impulse approximation (Spitzer 1958; Binney & Tremaine 1987). The energy imparted into a galaxy during a noninterpenetrating impulsive interaction can be computed in the tidal approximation by (Spitzer 1958),

$$\Delta {\rm E} = \frac{4G^2 M_2^2 M_1}{3b^4 V^2} r^2 , \quad (8)$$

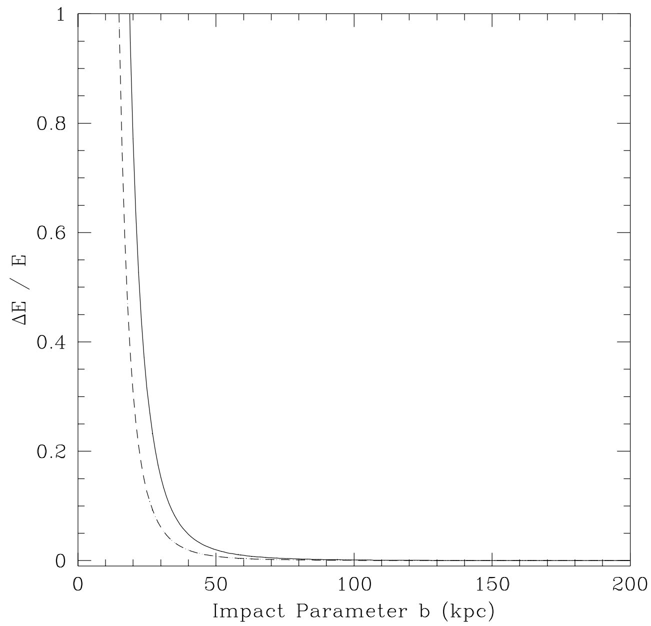

FIG. 11.—Ratio of the increase in internal energy produced in an impulsive interaction to the total internal energy, for two model galaxies as a function of the impact parameter *b*. For both a galaxy with a large size (5 kpc; *solid line*) and a smaller size (2 kpc; *dashed line*) the increase in internal energy is not enough to destroy the galaxy with impact parameters greater than ~ 30 kpc.

where M_1 and M_2 are the masses of two systems undergoing the impulse, b is the impact parameter, V is the initial relative velocity of the two systems, and r^2 is the mean-square radius of the perturbed system. This energy typically goes into the individual stars that can then be liberated from their host galaxies (Gallagher & Ostriker 1972; Aguilar & White 1985).

An important question to ask is if this internal energy addition will be enough to destroy individual galaxies. Figure 11 shows the ratio of ΔE to the internal energy, defined as $1/2\ M_1 \sigma^2$, of a galaxy interacting with a $M = 10^{12}\ M_\odot$ system, as a function of the impact parameter, b, from equation (8). Both lines represent systems with internal velocity dispersions $\sigma = 50$ km s^{-1} and relative velocity $V = 1000$ km s^{-1}, with the solid line a system with radius $r = 5$ kpc (a spiral) and the dashed line with radius $r = 2$ kpc (a dwarf). The ratio of the increase in internal energy from an impulsive interaction to the internal binding energy of a galaxy with velocity dispersion σ is given by

$$\frac{\Delta \mathrm{E}}{\mathrm{E}_{\mathrm{internal}}} = \frac{8}{3} \frac{G^2 M_2^2}{V^2 \sigma^2} \left(\frac{r^2}{b^4}\right) . \qquad (9)$$

Figure 11 shows the relative unimportance of this energy increase for destroying galaxies undergoing a single impulse. Typically only dwarf systems that come within 10 kpc of large ellipticals with mass $\sim 10^{12}\ M_\odot$ will receive enough of an increase in internal energy to disrupt the system in one encounter. These distances are rarely, if ever, reached in a cluster of galaxies such as Virgo. In addition, at this close distance the impulse approximation breaks down, and these equations no longer hold. The impulse energy from high-speed interactions is thus unlikely to destroy the large number of dwarf ellipticals in Virgo, at least on short timescales. This will, however, potentially have an important effect on each galaxy's internal evolution (see § 5.3).

5. DISCUSSION

In the previous section we demonstrated how dETs, along with the Virgo spirals, irregulars, and S0s, all have kinematic signatures of past accretion. In this section we discuss several possible origins of the Virgo dETs. This includes investigating whether or not dETs could be accreted field dwarfs, or whether they formed from some dynamical process induced by the cluster.

5.1. *Infalling Field and Group Dwarfs*

Could a significant fraction of Virgo dETs originate from field or group dEs accreted into Virgo? Is it possible that some or all the dETs in Virgo were once part of something like the Local Group (LG) that fell into Virgo, with the dETs dislodging from the spirals? The answer depends on the number of dwarfs in groups and in the field, an uncertain quantity (e.g., Ellis et al. 1996; Trentham 1998). We do, however, have some limits on the number of field dwarfs, and particularly the number of dwarf galaxies around spirals, such as those in the Local Group. The number of dwarf galaxies per giant is very high in clusters, much higher than in the field (e.g., Binggeli et al. 1990; Secker & Harris 1996). If all the spirals in Virgo originated in systems similar to the LG then in the magnitude limit of the VCC ($B_T \leq 18$; $M_B < -13.3$ assuming $m - M = 31.3$) there are only five LG dwarf spheroidals that could be detected. These are NGC 147, NGC 185, NGC 205, the Fornax dSph, and the Sagittarius dSph. We consider M32 a stripped giant elliptical, and not a dwarf elliptical, for these purposes, although including it as a dE does not change the following results.

There are only three bright LG spiral galaxies, and they are all detectable with the same magnitude limit: the Milky Way, M31, and M33. This gives a dwarf elliptical to giant spiral ratio of $5/3 = 1.67$. In the VCC there are 1277 members, with 574 more possible members, most of which are dwarf ellipticals. There are, however, only slightly over 100 spiral galaxies in Virgo (~ 160 if we include S0s), which would correspond to less than 300 detectable dwarf ellipticals if the dET/gS ratio were the same as in the LG. Similarly, if the 40 Virgo cluster ellipticals originated from mergers of spirals, they would also come from an initial population of ~ 100 spirals, and we would again expect to find only a few hundred dE companions. The VCC has well over 1000 dEs at these limits, and thus a simple scenario where the Virgo dEs are old members of galaxy groups dislodged from their spiral parents under predicts the number of dEs by over a factor of 3. There is also no sign of excess dEs associated with currently infalling spirals. Since the ratio of E/S0s to dEs is lower than that which see in groups, we conclude that dETs in clusters cannot be accounted for by accretion of field dEs or dwarfs attached to infalling spirals that later become removed.

5.2. *Gas Stripping: dI → dE*

One of the historically more popular methods of creating a dwarf elliptical is by stripping gas from a star-forming dwarf irregular (Lin & Faber 1981). This type of evolution is possible in Virgo since the dIs, along with the spirals, have an infalling signature and thus it is possible that a large number of dIs were accreted in the past. We do know that the large number of dETs cannot be accounted for by the relatively small number of present day dIs (Gallagher & Hunter 1989), and thus a much higher past dI accretion rate would be required. We therefore conclude that the vast majority of the dETs in this study, which are by necessity bright, did not evolve from irregulars. However, because of the huge population of cluster dETs and their large range in sizes and magnitudes, it seems possible that some of them, particularly the low-mass ones, evolved from irregulars. Irregulars have low masses and it is possible that after rapid gas stripping processes such as impulse encounters would produce a very small and faint dwarf elliptical after many Gyr. It would be very useful to extend searches for an extremely faint population of dEs that should exist, as products of the evolution of dIs that have been accreted into clusters over many epochs along with their spiral companions (Impey, Bothun & Malin 1988). Some of these have potentially been found in Virgo (Caldwell & Armandroff 2000).

5.3. *Galaxy Harassment:* $S \rightarrow dE$

Galaxy harassment (Moore et al. 1996, 1998) is the process whereby cluster galaxies are stripped of their interstellar medium and become dynamically "heated" by high-speed interactions with other cluster galaxies and the cluster's gravitational potential. During these encounters the internal potential energy of an infalling galaxy increases creating a situation where the galaxy is no longer in equilibrium. To reestablish equilibrium the galaxy increases in size and loses its most energetic stars. Because of this, the galaxy's density decreases over time, and after several orbits a spiral can morphologically transform into a dwarf elliptical (Moore et al. 1998). The lost mass necessarily becomes part of the intracluster material.

Galaxy harassment can explain a number of observations. Moderate redshift clusters at $z \sim 0.8$ have a high fraction of spirals and other star-forming galaxies (e.g., Butcher & Oemler 1978, 1984; Dressler et al. 1994; Oemler, Dressler, & Butcher 1997) that are not seen in the same frequency in nearby clusters. These blue galaxies typically do not have identifiable merging or interacting companions, and therefore could be products of high-speed interactions or galaxy interactions with the cluster potential inducing star formation. Features in nearby clusters, such as debris arcs (Mobasher & Trentham 1998; Gregg & West 1998) and distorted galaxies without obvious companions (Conselice & Gallagher 1999), are consistent with the harassment ideas of cluster galaxy evolution. The intracluster light in nearby clusters has colors similar to those of dwarf ellipticals, suggesting that material similar material from dwarfs, perhaps the remnant material from stripping, is the source of this light (e.g., Secker et al. 1997). Stripping is further confirmed by finding red giant branch stars (Ferguson, Tanvir, & von Hippel 1998) and planetary nebula (e.g., Mendez et al. 1997) in the Virgo cluster intragalactic regions.

The kinematic results presented here also support the galaxy harassment scenario for a dET origin. As shown in § 4, the velocity characteristics of low-mass ($<10^{10}$ $M_\odot$) infalling galaxies should change little over several gigayears, and thus their velocity and spatial distributions should reflect the mass profile of Virgo at the time of accretion (Carlberg et al. 1997). Galaxies accreted by more massive clusters will have higher observed velocities than those galaxies accreted by a lower mass cluster of the same size. If galaxies in Virgo were distributed in a similar way, those accreted early will have existed in the cluster longer, and thus they should be more dynamically stripped by high-speed interactions than those accreted recently. In this scenario accreted galaxies with the lowest masses should have the lowest velocity dispersions. After the giant ellipticals, the dS0s and dEs have the lowest velocity dispersions (Table 4), with a combined $\sigma = 621$ km s^{-1}. The S0s and dE,Ns, generally more massive than the dS0s and dEs, have a combined $\sigma \sim 705$ km s^{-1}, over 80 km s^{-1} higher than that of the lower mass dEs and dS0s. This difference and the difference in spatial distributions is potentially reflecting the different masses of Virgo when each galaxy type entered the cluster. This is also consistent with the spirals and irregulars infalling now, since these galaxies have a combined $\sigma \sim 756$ km s^{-1}, higher than any of the other galaxy types.

This, however, is circumstantial, since the cluster mass given by each population depends upon their spatial and velocity distributions. This can be investigated in detail by using the Jeans equation that relates orbital and spatial distributions of particles in a spherical system to that system's mass profile $M(r)$ (Binney & Tremaine 1987; Carlberg et al. 1997),

$$M(r) = -\frac{r \times v_r^2}{G} \times \left(\frac{d \ln \nu(r)}{d \ln r} + \frac{d \ln v_r^2}{d \ln r} + \beta\right), \quad (10)$$

where $\nu(r)$ is the radial density profile parameter, v_r^2 is the radial velocity dispersion, and β is the anisotropy parameter, $\beta = 1 - v_\theta^2/v_r^2$. It is impossible to derive the value of β without knowing the mass profile of Virgo, or to obtain the mass profile without an assumption about β. The luminosity density, ν, and total velocity dispersion, v^2, are real space quantities, while we observe the projected luminosity density N and projected velocity dispersion σ^2. Figure 12 shows the projected spatial distribution of various populations, and Table 7 list the projected slopes for both the velocity and spatial distributions. It is possible to convert these slopes into three-dimensional quantities by using the Abel transformation (e.g., Binney & Mamon 1982),

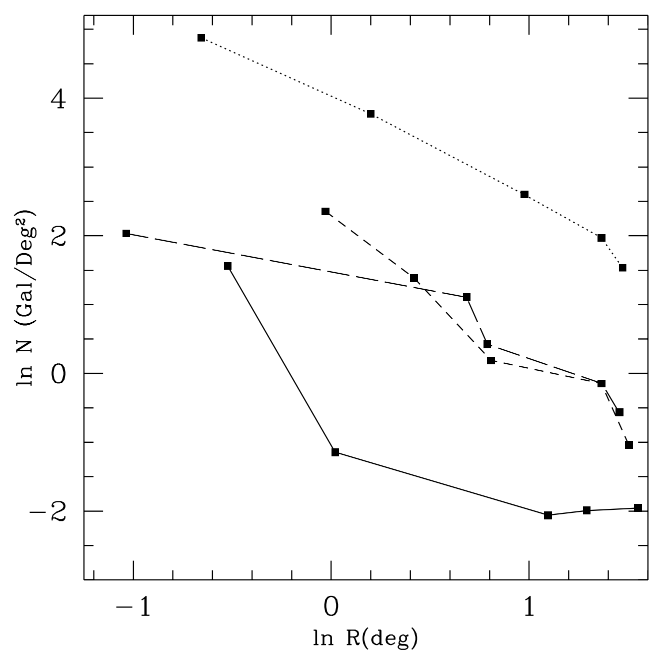

FIG. 12.—Projected spatial distribution, N, in galaxies per square degree as a function of radius. Ellipticals have the lowest densities and are represented by a solid line. The spirals are short-dashed lines, and irregulars long-dashed ones. The dETs, the densest population, are designated by the small dotted line.

TABLE 7

PROJECTED SPATIAL AND VELOCITY GRADIENT SLOPES

Type	$d \ln I/d \ln R$	$d \ln \sigma^2/d \ln R$
Ellipticals......	-2.04 ± 0.85	-0.45 ± 0.10
Irregulars......	-1.01 ± 0.22	-0.08 ± 0.11
dETs...........	-1.52 ± 0.10	-0.09 ± 0.05
Spirals	-2.01 ± 0.30	-0.06 ± 0.10

although we do not have enough information to do this. Additionally, only the dETs have a projected spatial distribution slope that can be measured with certainly out to a few degrees in radius.

Other recent evidence of S → dE evolution includes luminosity profiles of dEs and dE,Ns (Stiavelli et al. 2001), demonstrating that dETs have inner profiles more similar to spiral bulges than those of giant ellipticals. Many Virgo dETs also contain disklike, as opposed to elliptical-like, profiles (Ryden et al. 1999), and there are examples of Virgo dETs with faint spiral structure, including IC 3328 (Jerjen, Kalnajs, & Binggeli 2000). There are also Virgo dETs with dust and gas features commonly associated with late-type star-forming galaxies (Elmegreen et al. 2000). These observations all suggest that dETs could be descendents of star-forming disk galaxies.

How could so many cluster dEs (VCC) originate from spirals? The rate of infalling galaxies into clusters is predicted to peak at $z \sim 0.8$ in a CDM cosmology with $\Omega_M = 1$, $H_0 = 50$ km s^{-1} Mpc^{-1} (Kauffmann 1995). This is the same redshift at which the Butcher-Oemler effect is found and where the infall rates into clusters is observed to be high (Ellingson et al. 2001). If dEs originate from spirals, then a significant number of them should have been introduced into the cluster at approximately this redshift. Since dEs are galaxies with infall signatures, including a non-Gaussian velocity distribution, that cannot be intrinsic to an old cluster population, or to accreted field dEs, they likely originate from this epoch. They are therefore possibly the modern descendents of harassed Butcher-Oemler galaxies.

5.3.1. *dEs versus dE,Ns*

The velocity characteristics of dEs and dE,Ns are not significantly different (pure dEs are shaded in Figs. 4 and 5). This suggests that these two populations have similar origins and that dE,Ns are *not* scaled-down giant ellipticals. The one possible difference between dE and dE,Ns is their spatial distribution (Fig. 6), with the dE,Ns appearing more centrally concentrated in Virgo (Ferguson & Sandage 1989). Analysis of VCC positions for the dEs and dE,Ns shows that although the average distance from M87 is different by $0\overset{\circ}{.}31$ for the dEs ($2.25 \pm 1\overset{\circ}{.}73$) and the dE,Ns ($1.94 \pm 1\overset{\circ}{.}64$), this difference is not significant when we consider the large $\sim 1\overset{\circ}{.}7$ dispersions and when errors are taken into account.

Ferguson & Sandage (1989) found a luminosity dependence in clustering for Virgo dEs, such that dE,Ns and the faint nonnucleated dEs are centrally concentrated, but the bright nonnucleated dEs are not. There are several possibilities for explaining these trends. The nuclei of dE,Ns could be induced from gravitational effects due to the cluster core. This can occur in two ways. One could be a gravitational effect similar to the one producing the large fraction of barred spirals found in the Virgo core region (Andersen 1996), where tides could induce an increase in stellar density at the cores of dwarf galaxies. On the other hand the gravitational potential could also stabilize dEs in the central regions of Virgo, allowing globular clusters to accrete to the center by dynamical friction, forming nuclei (Hernandez & Gilmore 1998; Oh & Lin 2000; Lotz et al. 2001). In addition, about 20% of Virgo dEs have nuclei offset from their centers (Binggeli, Barazza, & Jerjen 2000). This is a possible indication that external gravitational fields are driving the nuclei to oscillate about galaxy centers, and thus playing a role in dE nuclei evolution.

Another possibility is that nucleation is produced by star formation induced in the centers of these galaxies after they are accreted into the cluster. Any spirals that orbit close to the center of the cluster will experience gravitational torques that could induce gas to inflow into a dE,N progenitor's center producing bursts of star formation. Nucleated dEs also have a higher specific globular cluster frequency than nonnucleated dEs (Miller et al. 1998), an observation explainable by increased star formation in dE,N progenitors that orbit close to the Virgo core.

These observations suggest that the harassment process of transforming spirals into dEs is likely occurring, but probably is not the only source of these galaxies. Since most galaxies are in groups, and these fall into clusters, it seems certain that *some* dEs in Virgo were formed outside the cluster in galaxy groups. Our observations similarly do not rule out the possibility that some dEs in the core of Virgo were present when the cluster Es formed.

6. SUMMARY AND DISCUSSION

In this paper we derive the following conclusions based on the kinematic properties of Virgo cluster galaxies:

1. Elliptical galaxies in the Virgo core region form a relaxed, or nearly relaxed system. This is demonstrated by the Gaussian velocity distribution of the ellipticals and their centrally concentrated spatial distribution. No other galaxy population has characteristics of relaxation. This includes the S0s, dEs, dE,Ns, dS0s, as well as the spiral and irregular galaxies. Relaxation and dynamical friction are shown to be inefficient for significantly decreasing the velocity dispersion of galaxies with masses lower than $10^{10}\ M_{\odot}$, although these are potentially important for the ellipticals. Infalling galaxies should therefore retain their kinematic signatures even after many cluster crossings.

2. All populations, except for the ellipticals, have similar velocity dispersions (Table 4), with an average $\sigma_{\rm pop}/\sigma_{\rm E} = 1.49$, close to the expected ratio of velocity dispersions for a marginally bound and virialized population. The dET, S0, spiral and irregular galaxies have spatial distributions that are progressively less centrally concentrated and have increasingly non-Gaussian velocity distributions. We therefore conclude that most galaxy populations in Virgo, besides the giant ellipticals, have been accreted into the cluster after the giant Es were in place.

3. We investigate several possible origins for the dEs in Virgo including dislodging of dEs companions connected to infalling spiral hosts, transformation of infalling dIs into dEs, and stripping of material from infalling galaxies through processes such as harassment. We favor the last scenario with its implication that accreted spiral galaxies in the past were transformed into modern cluster dETs. This is suggested in part: the least massive galaxies, and those pre-

dicted to be the most stripped (dS0s and dETs) have the lowest velocity dispersion (621 km s^{-1}) of any population besides the large ellipticals. The spirals and irregulars, the newest additions to the cluster, have a combined $\sigma = 756$ km s^{-1}, the highest for any population, potentially reflecting the higher mass of Virgo when the dE progenitors were accreted. To confirm this will require a better understanding of the velocity anisotropy of the various galaxy populations and their three-dimensional spatial distributions.

These results have several implications. First, most dETs in clusters are not primordial cluster galaxies or galaxies that have existed since the large ellipticals were in place. Since dETs are common in clusters, have dynamical properties that suggest they were accreted by Virgo several Gyrs ago, and were more massive in the past, they are potentially the remnants of Butcher-Oemler galaxies. This raises the question of what happened to the original cold dark matter objects? Did they *all* merge early to form the giant elliptical population, or is there a large population of objects with masses and sizes similar to dEs, but with low surface brightness, that remain undetected (Cen 2001), or was the formation of low-mass halos suppressed (Bullock, Kravtsov, & Weinberg 2001)? Either solution for explaining away the lack of detected old low-mass cluster objects has deep implications for observational cosmology and deserves further attention.

This study suggests that many cluster dEs are fundamentally different from dwarf ellipticals, or dwarf spheroidals, found in groups, although they could both be produced by harassment (Mayor et al. 2001). Establishing whether this is true will require more observational evidence to show conclusively, but there may be two ways to form dEs—a simple galaxy collapse (e.g., Dekel & Silk 1986), and stripped down galaxies as suggested here. This paper also demonstrates how galaxy evolution can affect cosmological measurements. Galaxy clusters would be brighter if harassment did not occur, since galaxies are stripped of their stellar material. As a result this can change our estimate of cosmological biasing in dense regions.

Future papers in this series will explore the properties of the stellar populations in cluster dEs themselves to learn more about their histories and to identify exactly what their ancestors were. If cluster dEs are "primordial" cluster members then their stars should all have roughly the same age, with no star formation after their initial creation, owing to ram-pressure effects. If cluster dEs form by some other process, such as harassment of infalling spirals that were once BO galaxies, then there should be significant intermediate or young stellar populations. The stellar population ages of dEs should also correlate with their orbital kinematics.

We thank Linda Sparke, Harry Ferguson, Sydney Barnes, Gus Oemler, and Elizabeth Praton for comments and suggestions regarding this work. We also thank Bruno Binggeli for the electronic version of the VCC. The referee, Bryan Miller, raised several issues that improved the presentation of this paper. This research was supported in part by the National Science Foundation (NSF) through grants AST-980301 to the University of Wisconsin-Madison and AST-9804706 to Johns Hopkins University. C. J. C. acknowledges support from a Grant-In-Aid of Research from Sigma Xi and the National Academy of Sciences (NAS) as well as a Graduate Student Researchers Program (GSRP) Fellowship from NASA and a Graduate Student Fellowship from the Space Telescope Science Institute (STScI).

REFERENCES

Aguilar, L. A., & White, S. D. M. 1985, ApJ, 295, 374
Andersen, V. 1996, AJ, 111, 1805
Babul, A., & Rees, M. J. 1992, MNRAS, 255, 346
Balogh, M. L., Navarro, J. F., & Morris, S. L. 2000, ApJ, 540, 113
Bertin, G. 2000, Dynamics of Galaxies (New York: Cambridge Univ. Press
Binggeli, B., Barazza, F., & Jerjen, H. 2000, A&A, 359, 447
Binggeli, B., & Jerjen, H. 1998, A&A, 333, 17
Binggeli, B., Popescu, C. C., & Tammann, G. A. 1993, A&AS, 98, 275
Binggeli, B., Sandage, A., & Tammann, G. A. 1985, AJ, 90, 1681 (VCC)
Binggeli, B., Tammann, G. A., & Sandage, A. 1987, AJ, 94, 251
Binggeli, B., Tarenghi, M., & Sandage, A. 1990, A&A, 228, 42
Binney, J., & Mamon, G. A. 1982, MNRAS, 200, 361
Binney, J., & Tremaine, S. 1987, Galactic Dynamics (Princeton: Princeton Univ. Press)
Bothun, G. D., & Mould, J. R. 1988, ApJ, 324, 123
Bothun, G. D., Mould, J. R., Caldwell, N., & MacGillivray, H. T. 1986, AJ, 92, 1007
Bothun, G. D., Mould, J. R., Wirth, A., & Caldwell, N. 1985, AJ, 90, 697
Bullock, J. S., Kravtsov, A. V., & Weinberg, D. H. 2001, ApJ, 548, 33
Butcher, H., & Oemler, A., Jr.1978, ApJ, 219, 18
———. 1984, ApJ, 285, 426
Caldwell, N., & Armandroff, T. A. 2000, BAAS, 197, 106.05
Cayatte, V., Balkowski, C., van Gorkom, J. H., & Kotanyi, C. 1990, AJ, 100, 604
Carlberg, R. G., et al. 1997, ApJ, 476, 7L
Cen, R. 2001, ApJ, 546, 77L
Chandrasekhar, S. 1942, Principles of Stellar Dynamics (New York: Dover)
Colless, M., & Dunn, A. M. 1996, ApJ, 458, 435
Conselice, C. J., & Gallagher, J. S. 1999, AJ, 117, 75
Crone, M. M., Evrard, A. E., & Richstone, D. O. 1994, ApJ, 434, 402
Davies, R. L., Efstathiou, G., Fall, S. M., Illingworth, G., & Schechter, P. L. 1983, ApJ, 266, 41
Dekel, A., & Silk, J. 1986, ApJ, 303, 39
de Propris, R., Pritchet, C. J., Harris, W. E., & McClure, R. D. 1995, ApJ, 450, 534
de Vaucouleurs, G. 1961, ApJS, 6, 213
de Vaucouleurs, G., & de Vaucouleurs, A. 1973, A&A, 28, 109
de Vaucouleurs, G., de Vaucouleurs, A., Corwin, J. R., Buta, R. J., Paturel, G., & Fouque, P. 1991, The Third Reference Catalog of Bright Galaxies (New York: Springer)
Diaferio, A., Kauffmann, G., Balogh, M. L., White, S. D. M., Schade, D., & Ellingson, E. 2001, MNRAS, 323, 999
Dressler, A. 1984, ARA&A, 22, 185
Dressler, A., Oemler, A. Jr., Gunn, J. E., & Butcher, H. 1994, ApJ, 404, L45
Dressler, A., et al. 1997, ApJ, 490, 577
Drinkwater, M. J., Currie, M. J., Young, C. K., Hardy, E., & Yearsley, J. M. 1996, MNRAS, 279, 595
Duprie, K., & Schneider, S. E. 1996, AJ, 112, 937
Ellingson, E., Lin, H., Yee, H. K. C., & Carlberg, R. G. 2001, ApJ, 547, 609
Ellis, R. S., Colless, M., Broadhurst, T., Heyl, J., & Glazebrook, K. 1996, MNRAS, 280, 235
Ellis, R. S., Smail, I., Dressler, A., Couch, W. J., Oemler, A., Jr., Butcher, H., & Sharples, R. M. 1997, ApJ, 483, 582
Elmegreen, D. M., Elmegreen, B. G., Chromey, F. R., & Fine, M. S. 2000, AJ, 120, 733
Farooqui, S. Z. 1994, Ph.D. thesis, Univ. Texas
Ferguson, H. C. 1992, MNRAS, 255, 389
Ferguson, H. C., & Binggeli, B. 1994, A&A Rev., 6, 67
Ferguson, H. C., & Sandage, A. 1988, AJ, 96, 1520
———. 1989, ApJ, 346, 53L
Ferguson, H. C., Tanvir, N. R., & von Hippel, T. 1998, Nature, 391, 461
Gallagher, J. S., III, & Hunter, D. A. 1989, AJ, 98, 806
Gallagher, J. S., III, & Ostriker, J. P. 1972, AJ, 77, 288
Gallagher, J. S., III, & Wyse, R. F. G. 1994, PASP, 106, 1225
Gavazzi, G., Boselli, A., Scodeggio, M, Pierini, D., & Belsole, E. 1999, MNRAS, 304, 595
Giraud, E. 1999, ApJ, 524L, 15
Gott, J. R., III, Rees, M. J. 1975, A&A, 45, 365
Governato, F., Ghigna, S., Moore, B., Quinn, T., Stadel, J., & Lake, G. 2001, ApJ, 547, 555
Grebel, E. K. 2000, in Star Formation from the Small to the Large Scale, 33rd ESLAB Symp., ed. F. Favata, A. A. Kaas, & A. Wilson (ESA SP-445; Noordwijk: ESA), 87

Gregg, M. D., & West, M. J. 1998, Nature, 396, 549
Grogin, N. A., Geller, M. J., & Huchra, J. P. 1998, ApJS, 119, 277
Haynes, M. P., & Giovanelli, R. 1986, ApJ, 306, 466
Held, E. V., & Mould, J. R. 1994, AJ, 107, 1307
Hernandez, X., & Gilmore, G. 1998, MNRAS, 297, 517
Ho, L. C., Filippenko, A. V. Sargent, W. L. W., & Peng, C. Y. 1997, ApJS, 112, 391
Hodge, P. W. 1959, PASP, 71, 28
———. 1960, PASP, 72, 188
———. 1965, AJ, 70, 559
Hoffman, G. L., Salpeter, E. E., Farhat, B., Roos, T., Williams, H., & Helou, G. 1996, ApJS, 105, 269
Holmberg, E. 1961, AJ, 66, 620
Huchra, J. 1985, in ESO Workshop on the Virgo Cluster, ed. O.-G. Richter & B. Binggeli (Garching: ESO), 191
Huchra, J., Davis, M., Latham, D., & Tonry, J. 1983, ApJS, 52, 89
Impey, C., Bothun, G., & Malin, D. 1988, ApJ, 230, 634
James, P. 1991, MNRAS, 250, 544
Jerjen, H., Kalnajs, A., & Binggeli, B. 2000, A&A, 358, 845
Kauffmann, G. 1995, MNRAS, 274, 153
———. 1996, MNRAS, 281, 487
Koo, D. C., Guzman, R., Faber, S. M., Illingworth, G. D., Bershady, M. A., Kron, R. G., & Takamiya, M. 1995, ApJ, 440L, 49
Koo, D. C., Guzman, R., Gallego, J., & Wirth, G. D. 1997, ApJ, 478L, 49
Koopmann, R. A., & Kenney, J. D. P. 1998, ApJ, 497L, 75
Kurtz, M., & Douglas, J. 1998, PASP, 110, 934
Lee, H., Richer, M. G., & McCall, M. L. 2000, ApJ, 530, 17L
Lin, D. N. C., & Faber, S. M. 1983, ApJ, 266L, 21
Lotz, J. M., Telford, R., Ferguson, H. C., Miller, B. W., Stiavelli, M., & Mack, J. 2001, ApJ, 552, 572
Mahdavi, A., Geller, M. J., Böhringer, H., Kurtz, M. J., & Ramella, M. 1999, ApJ, 518, 69
Mao, S., & Mo, H. J. 1998, MNRAS, 296, 877
Marquardt, D. W. 1963, J. SIAM, 11, 431
Marzke, R., & da Costa, L. N. 1997, AJ, 113, 185
Mateo, M. L. 1998, ARA&A, 36, 435
Mayor, L., Governato, F., Colpi, M., Moore, B., Quinn, T., Wadsley, J., Stadel, J., & Lake, G. 2001, ApJ, 547, 123L
Mendez, R. H., Guerrero, M. A., Freeman, K. C., Arnaboldi, M., Kudritzki, R. P., Hopp, U., Capaccioli, M., & Ford, H. 1997, ApJ, 491, L23
Michard, R., & Marchal, J. 1994, A&AS, 105, 481
Miller, B., Lotz, J., Ferguson, H., Stiavelli, M., & Whitmore, B. C. 1998, ApJ, 508, L133
Mobasher, B., & Trentham, N. 1998, MNRAS, 293, 315
Moore, B., Katz, N., Lake, G., Dressler, A., & Oemler, A., Jr. 1996, Nature, 379, 613
Moore, B., Lake, G., & Katz, N. 1998, ApJ, 495, 139
Moore, B., Lake, G., Quinn, T., & Stadel, J. 1999, MNRAS, 304, 465
Mori, M., & Burkert, A. 2000, ApJ, 538, 599
Neilsen, E. H., Jr., & Tsvetanov, Z. I. 2000, ApJ, 536, 255
Oemler, A., Jr., Dressler, A., & Butcher, H. R. 1997, ApJ, 474, 561
Oh, K. S., & Lin, D. N. C. 2000, ApJ, 543, 620
Okamoto, T., & Nagashima, M. 2001, ApJ, 547, 109
Ostriker, J. A. 1993, ARA&A, 31, 589
Peebles, P. J. E. 1980, The Large-scale Structure of the Universe (Princeton: Princeton Univ. Press)
Phillipps, S., Parker, Q. A., Schwartzenberg, J. M., & Jones, J. B. 1998, ApJ, 493, L59
Praton, E. A., & Schneider, S. E. 1994, ApJ, 422, 46
Press, W. H., Teukolsky, S. A., Vetterling, W. T., & Flannery, B. P. 1992, Numerical Recipes (Cambridge: Cambridge Univ. Press)
Reeves, G. 1956, AJ, 61, 69
———. 1977, AJ, 89, 620
Rubin, V. C., Waterman, A. H., & Kenney, J. D. P. 1999, AJ, 118, 236
Ryden, B. S., Terndrup, D. M., Pogge, R. W., & Lauer, T. R. 1999, ApJ, 517, 650
Schindler, S., Binggeli, B., & Böhringer, H. 1999, A&A, 343, 420 (SBB)
Secker, J., & Harris, W. E. 1996, ApJ, 469, 623
Secker, J., Harris, W. E., & Plummer, J. D. 1997, PASP, 109, 1377
Smith, S. 1936, ApJ, 83, 23
Solanes, J. M., Manrique, A., Garcia-Gomez, C., Gonzalez-Casado, G., Giovanelli, R., & Haynes, M. P. 2001, ApJ, 548, 97
Spitzer, L. 1958, ApJ, 127, 17
———. 1987, Dynamical Evolution of Globular Clusters (Princeton: Princeton Univ. Press)
Spitzer, L., & Hart, M. 1971, ApJ, 171, 399
Stiavelli, M., Miller, B. W., Ferguson, H. C., Mack, J., Whitmore, B. C., & Lotz, J. M. 2001, ApJ, 121, 1385
Strauss, M. A., Huchra, J. P., Davis, M., Yahil, A., Fisher, K., & Tonry, J. 1992, AJ, 83, 29
Sullivan, M., Treyer, M. A., Ellis, R. S., Bridges, T. J., Milliard, B., & Donas, J. 2000, MNRAS, 312, 442
Thomas, P. A., et al. 1998, MNRAS, 296, 1061
Tonry, J., & Davis, M. 1979, AJ, 84, 1511
Trentham, N. 1997, MNRAS, 286, 133
———. 1998, MNRAS, 293, 71
van den Bergh, S. 2000, The Galaxies in the Local Group (Cambridge: Cambridge Univ. Press)
van den Bosch, F. C., Ferrarese, L., Jaffe, W., Ford, H. C., & O'Connell, R. W. 1994, AJ, 108, 1579
White, S. D. M., & Frenk, C. S. 1991, ApJ, 379, 52
White, S. D. M., & Springel, V. 1999, preprint astro-ph/9911378
Young, C. K., & Currie, M. J. 1995, MNRAS, 273, 1141
Zabludoff, A. I., & Mulchaey, J. S. 1998, ApJ, 496, 39
Zwicky, F. 1933, Helvetica Phys. Acta., 6(2), 110